

超新星爆発とニュートリノ

鈴木英之

東京理科大学理工学部物理学科

超新星爆発

Type Ia: 白色矮星の核燃焼暴走による超新星爆発

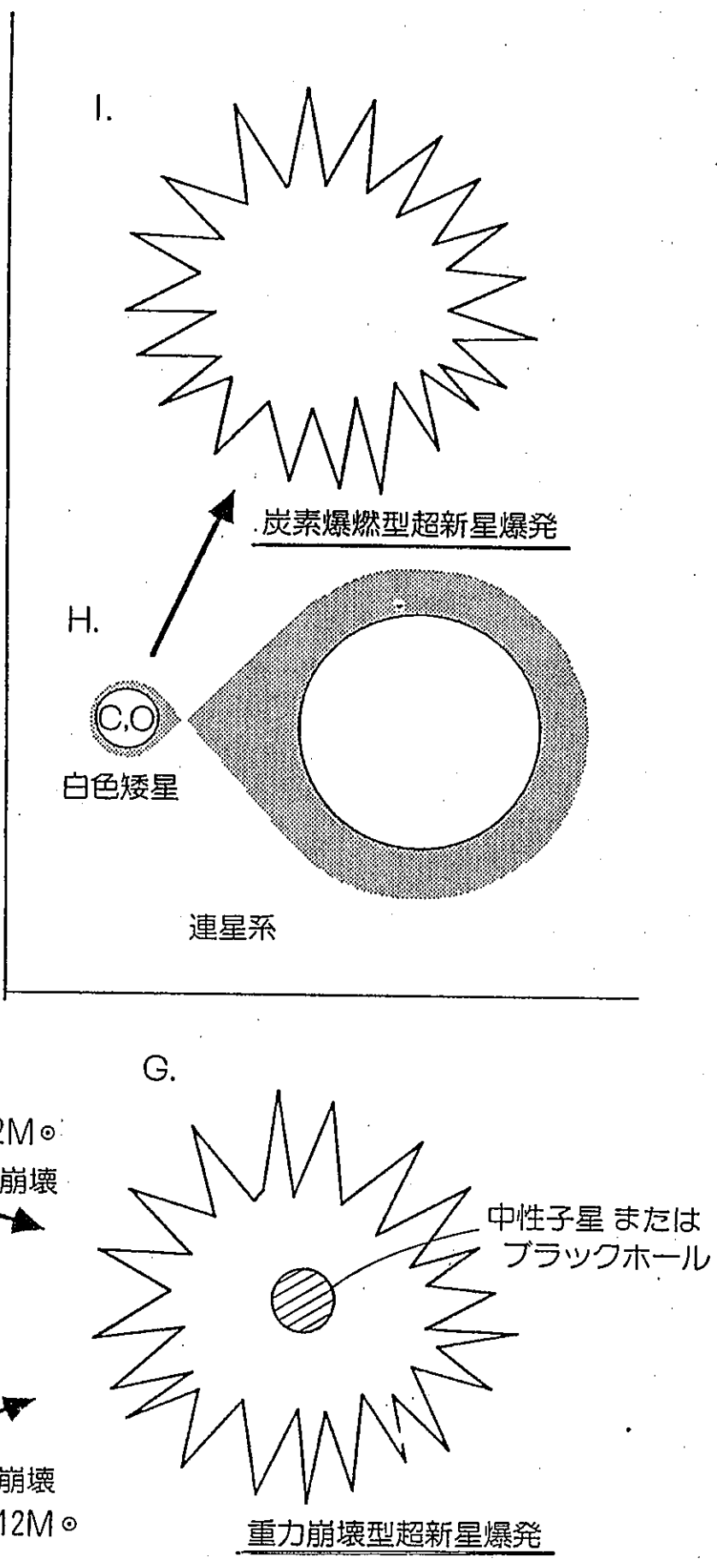
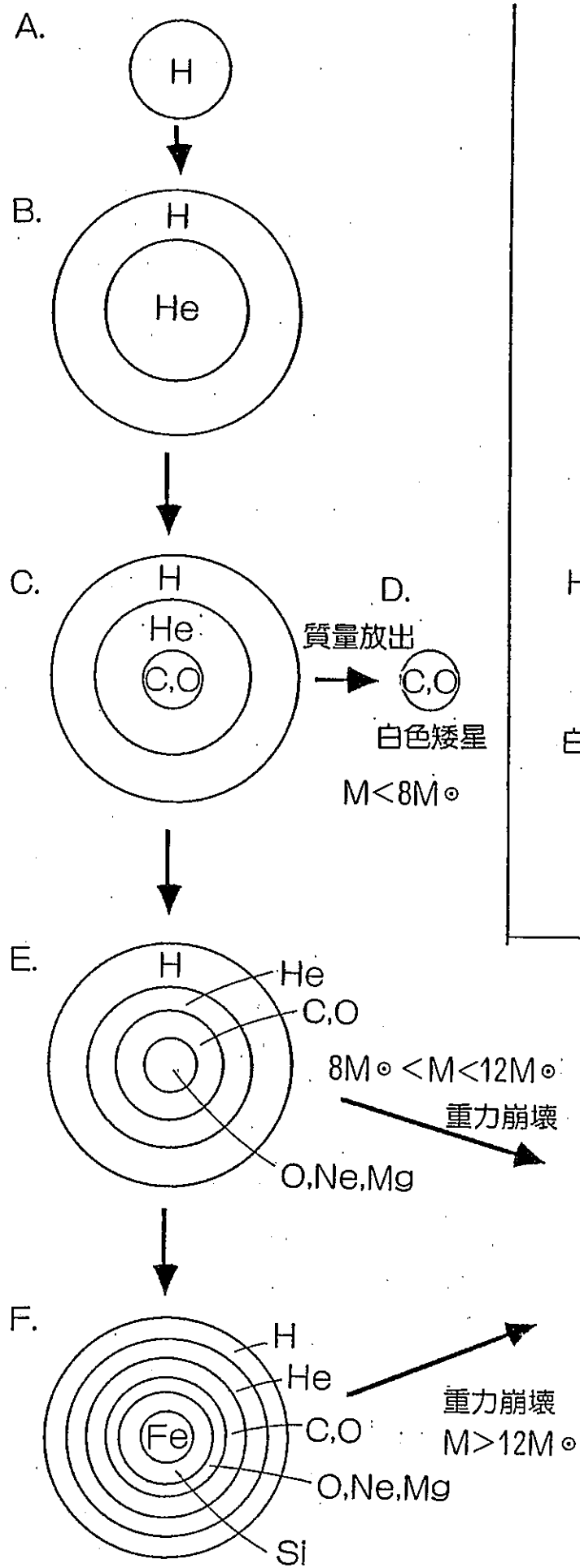
no compact remnant

宇宙論の標準光源?

Type Ib,Ic,II: 重い星のコアの重力崩壊による超新星爆発

中性子星・ブラックホールの形成

ニュートリノバースト



1 重力崩壊型超新星爆発のシナリオ

- 重力崩壊前のコア (Fe or O·Ne·Mg core)

$$M_{\text{core}} = 1 \sim 2 M_{\odot}, \quad M_{\text{主系列}} > 8 M_{\odot}$$

$$R_{\text{core}} = 10^8 \sim 10^9 \text{cm}, \quad R_{\text{star}} = 10^{12} \sim 10^{14} \text{cm}$$

$$\rho_c = 10^9 \sim 10^{10} \text{g/cm}^3 \sim 10^{-5} \rho_{\text{nuc}}$$

$$T_c = 0.1 \sim 1 \text{MeV}, \quad S \sim O(1)$$

$$\mu_e = 11.1 \text{MeV} \left(\frac{\rho Y_e}{10^{10} \text{g/cm}^3} \right)^{1/3} \gg m_e, T : \text{rel. deg. electrons}$$

$$e^- A \longrightarrow \nu_e A' : \lambda_\nu \gg R_{\text{core}} \text{ freely escape}$$

- Onset of core collapse

電子捕獲 (electron capture) $e^- A \longrightarrow \nu_e A'$, $\lambda_\nu \gg R_{\text{core}}$

光分解 (photodissociation) $^{56}\text{Fe} \gamma \longrightarrow 13^4\text{He} 4n - 125 \text{MeV}$

dynamical time scale: $\tau_{\text{dyn}} \sim 1/\sqrt{G\rho} \sim 40 \text{msec} \left(\frac{\rho}{10^{10} \text{g/cm}^3} \right)^{-1/2}$

- Nuclear Statistical Equilibrium

- ν trapping ($\rho > 10^{10} - 10^{12} \text{ g/cm}^3$)

ν_e from $e^- A \longrightarrow \nu_e A'$ and $e^- p \longrightarrow \nu_e n$

main opacity source: coherent scattering $\nu_e A \longrightarrow \nu_e A$

cross section $\sigma \propto A^2 \omega_\nu^2$

重力崩壊の進行にともない

$\lambda_\nu < R_{\text{core}}$: 不透明に (neutrinosphere の出現)

diffusion time scale of neutrinos: $\tau_{\text{diff}} = 3R_{\text{core}}^2/c\lambda_\nu > \tau_{\text{dyn}}$

重力崩壊中にニュートリノはコアから出てこられない

= ニュートリノの閉じ込め (neutrino trapping)

ν_e 縮退 \implies suppression of $\begin{cases} \text{electron capture} \\ \text{neutronization of nuclei} \\ \text{neutron drip} \\ (\text{e.g. } X_A > 0.7 \text{ Bruenn 1985}) \end{cases}$

閉じ込め領域では

$$\nu_e A \longleftrightarrow e^- A', \quad \nu_e n \longleftrightarrow e^- p$$

$$\nu_e e^- \longrightarrow \nu_e e^- \text{ (down scattering: } \omega_\nu \searrow, \lambda_\nu \nearrow)$$

$$Y_{L\text{trap}} = 0.3 \sim 0.4$$

- バウンス、衝撃波の生成

$\rho_c > \rho_{\text{nuc}}$: 状態方程式が固くなる(核力のハードコア成分)
 バウンスした内部コア + 超音速で落下する外部コア
 バウンスした内部コアの境界領域で衝撃波が発生

$$M_{\text{i.c.}} \sim 1.457 M_{\odot} \left(\frac{Y_{L\text{trap}}}{0.5} \right)^2 = 0.6 \sim 0.9 M_{\odot}$$

$$E_{\text{shock}} \sim \frac{GM_{\text{i.c.}}^2}{R_{\text{i.c.}}} \propto Y_{L\text{trap}}^{10/3} \sim \text{several } 10^{51} \text{ erg}$$

$$> E_{\text{SNE}}(\text{kinetic + radiation}) \sim 10^{51} \text{ erg}$$

$$R_{\text{shock}} < R_{\nu\text{sphere}}$$

バウンスした内部コアは静水圧平衡状態に
 \Rightarrow 原始中性子星 (PNS: protoneutron star)

$$S_c \sim O(1), T_c \sim O(10) \text{ MeV}, Y_e \sim 0.3$$

- 衝撃波が neutrinosphere を通過

衝撃波の通過した領域では $A \rightarrow np$, $e^- p \rightarrow n \nu_e$ が進行
 $\sigma(e^- A \rightarrow \nu_e A') < \sigma(e^- p \rightarrow \nu_e n)$

$r(\text{shock}) < r(\nu \text{sphere})$: 生成された ν_e は trap されたまま
 $r(\text{shock}) > r(\nu \text{sphere})$: 生成された ν_e は自由に出てこられる
 main opacity source だった原子核も分解される
 $\Rightarrow \nu_e$ の中性子化バースト (neutronization burst)

$$\tau_{\text{neutronization burst}} \sim \tau_{\text{shock propagation}} \lesssim 10 \text{ msec}$$

$$L_{\nu_e \text{neutronization burst}} \gtrsim 10^{53} \text{ erg/sec}$$

$$\int L_{\nu_e \text{neutronization burst}} dt \sim 10^{51} \text{ erg}$$

Y_e 分布に deep trough を形成し、衝撃波を弱める。

- 外部コア内の衝撃波の伝播

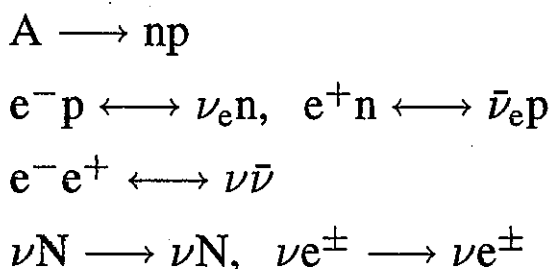
障害物

- ram pressure of falling matter
- 原子核の光分解(吸熱反応)
- 自由陽子による電子捕獲(圧力低下)
- ニュートリノ放出によるエネルギー損失
($R_{\nu\text{sphere}} < r < R_{\text{shock}}$)

衝撃波は?

コア表面に無事到達 \Rightarrow prompt explosion ($\tau \sim O(10)\text{msec}$)
$r \sim \text{数 } 100\text{km}$ で停滞 $E(\text{dissociation}) \sim 8 \cdot 10^{51}\text{erg} \left(\frac{M_{\text{Fe core}} - M_{\text{i.c.}}}{0.5M_{\odot}} \right)$

In the shocked region ($S \sim O(10)$)



静水圧平衡の原始中性子星に、衝撃波の通過した外部コアの物質が降り積もる

$$M_{\text{PNS}} = M_{\text{i.c.}} (\sim 0.7M_{\odot}) \longrightarrow M_{\text{NS}} (\sim 1.4M_{\odot})$$

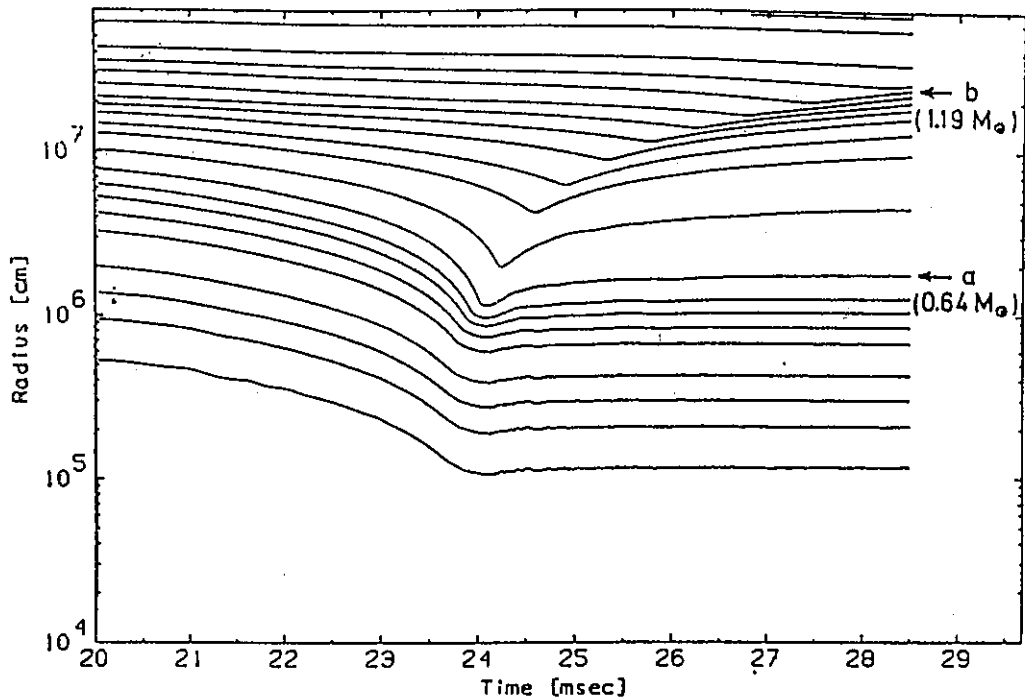


Figure 10: Successful prompt explosion ($M_{\text{main sequence}} = 9M_{\odot}$). Lines are trajectories of selected mass zones (taken from Hillebrandt, Nomoto & Wolff 1984 [57]). The point 'a' is the boundary of the unshocked inner core. The shock wave successfully propagates to the core surface and the material above the point 'b' will be blown off.

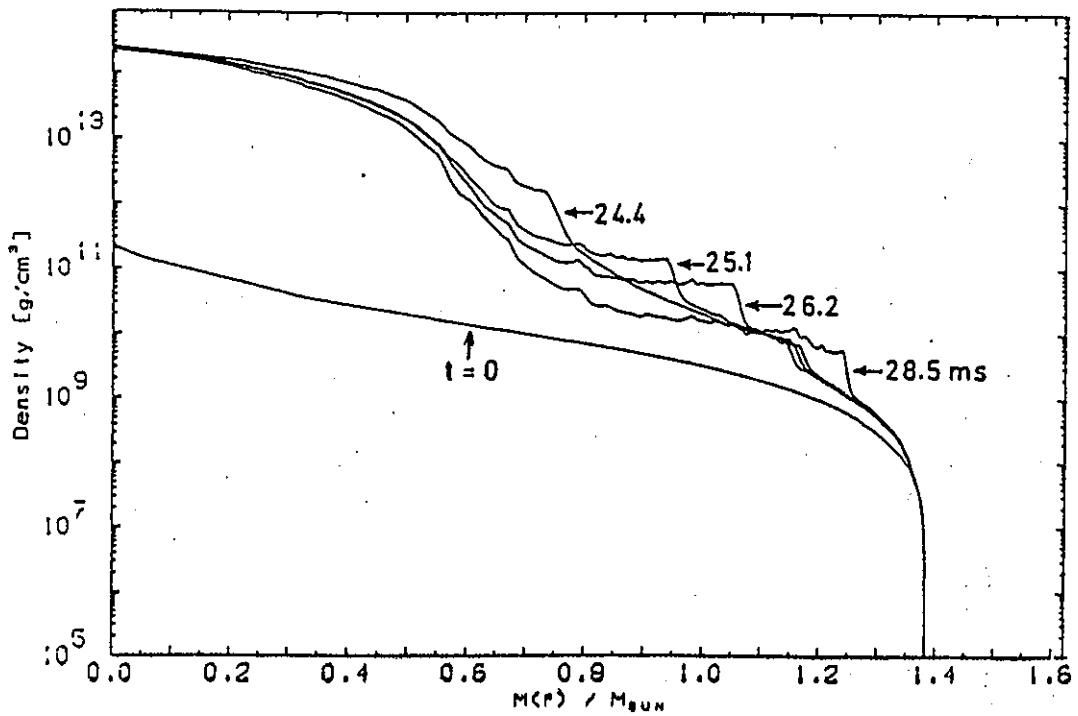


Figure 11: Successful prompt explosion: snapshots of density profile at selected times (initial model and shock propagating phase). $M_{\text{main sequence}} = 9M_{\odot}$ (taken from Hillebrandt, Nomoto & Wolff 1984 [57]).

Stalled Shock Wave

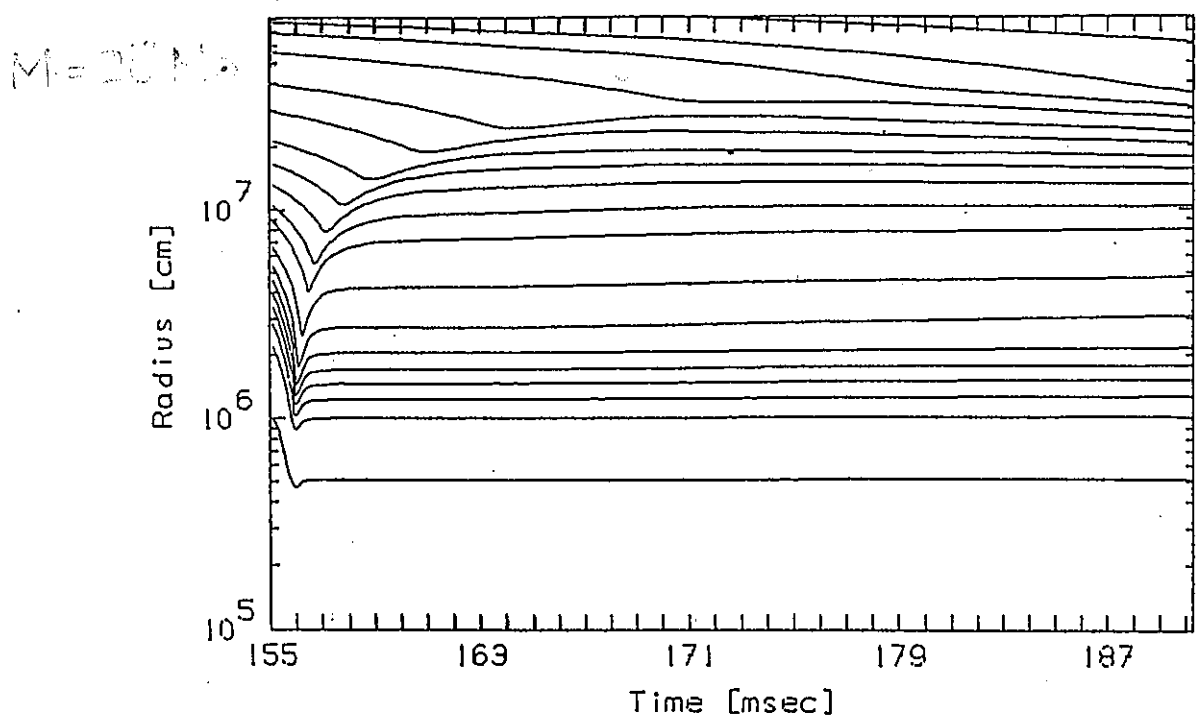


Figure 6: Radius versus time for selected mass zones of a $20M_{\odot}$ stellar model. Due to the large iron core no prompt explosion was observed.

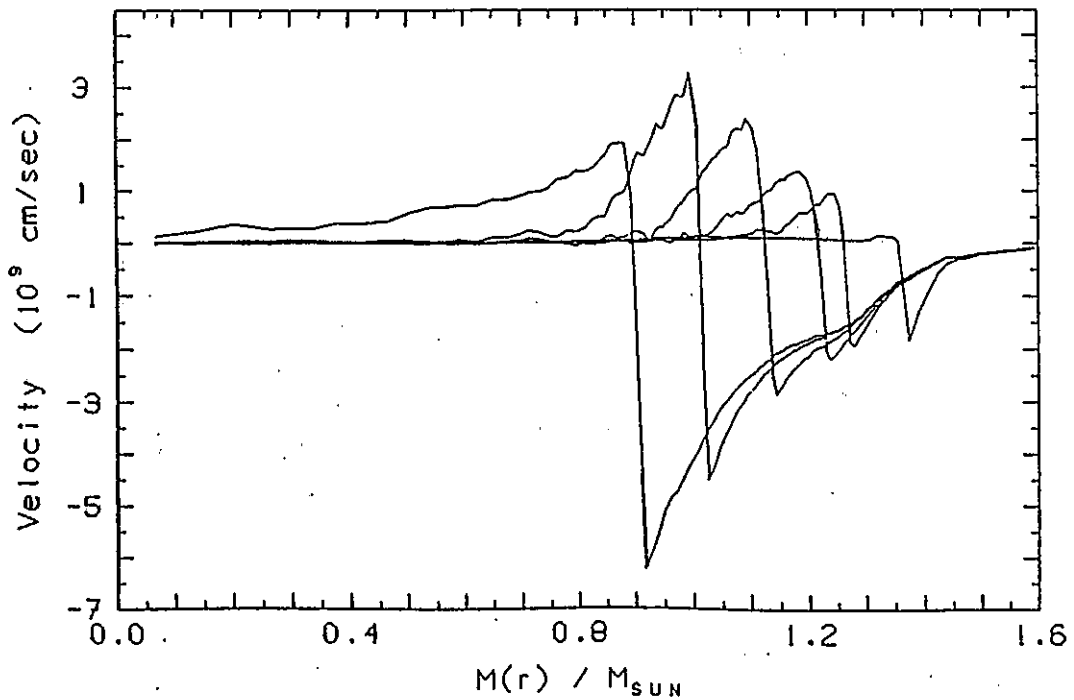
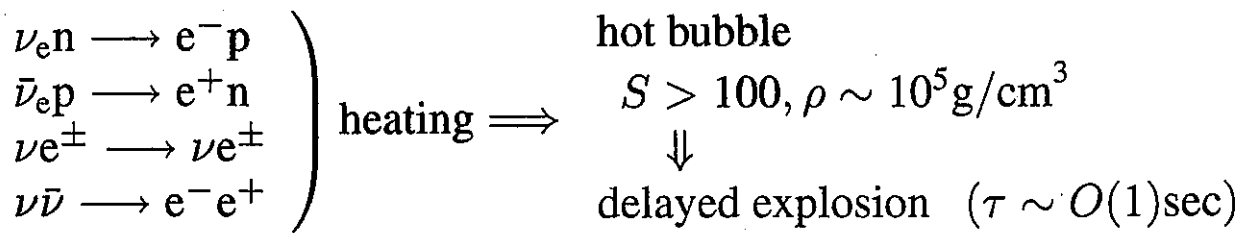


Figure 7: Snap-shots of velocities of a $20M_{\odot}$ model. Due to photo-dissociation of heavy nuclei the shock stagnates at about $1.3M_{\odot}$.

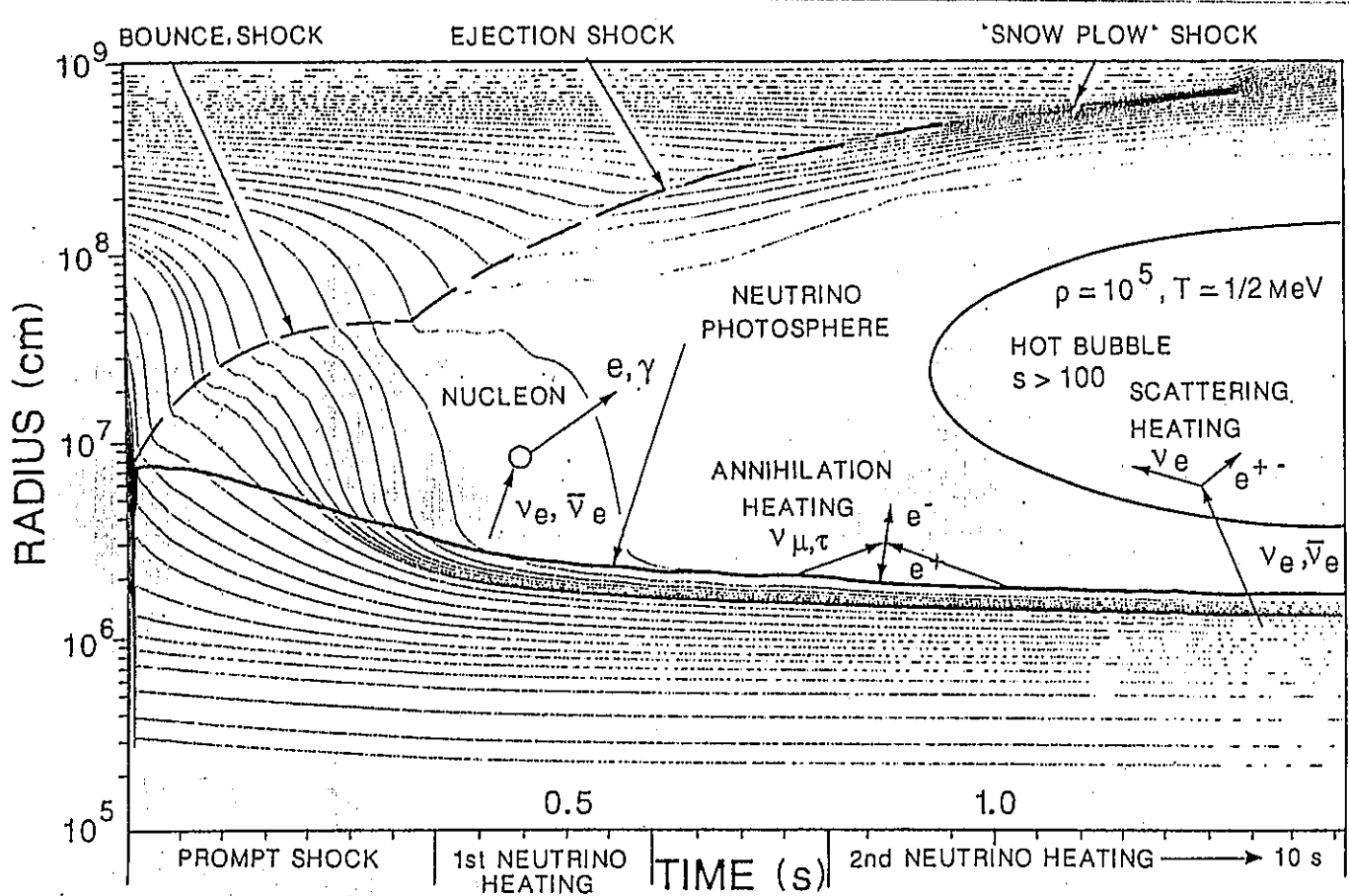
- 停滯した衝撃波の復活

原始中性子星からのニュートリノ $T_\nu \sim \text{数 MeV}$
shocked matter ($r \sim \text{数 } 100\text{km} > R_{\nu\text{sphere}}$) $T \sim \text{MeV}$



非球対称性が重要?

- 流体不安定性
- 回転



The sequence of processes occurring in a type II supernova according to Wilson and Mayle. First a star collapses, owing to exhaustion of the fuel and emits electron neutrinos as the compressing matter turns into neutrons. The forming neutron star bounces producing a strong shock that weakens owing both to the thermal decomposition of nuclear matter and the reversal of the neutron star bounce trajectory. Subsequently, a large burst of neutrinos of all flavours heats the infalling matter, starting an explosive shock. Yet later, mu and tau neutrino-antineutrino annihilations in nearly opposed collisions just above the neutrino photosphere generate heat without nucleonic matter, making a hot, high-entropy (100 Boltzmann-unit) bubble, which pushes out the ejected matter in a near 'snow plow', that is, a thin shock. The pressure is maintained because the high-entropy ensures a large scale height adjacent to the neutron star.

対流不安定性

Ledoux の不安定条件

$$\left(\frac{\partial \rho}{\partial \ln Y_L} \right)_{S,P} \frac{\partial \ln Y_L}{\partial r} + \left(\frac{\partial \rho}{\partial \ln S} \right)_{Y_L,P} \frac{\partial \ln S}{\partial r} > 0$$

$$\left(\frac{\partial \rho}{\partial \ln S} \right)_{Y_L,P} < 0$$

$$\left(\frac{\partial \rho}{\partial \ln Y_L} \right)_{S,P} \leq 0 \quad (\text{EOS や } \rho, S, P \text{ による})$$

cf. Shen EOS では、small Y_e high ρ で正

+ ニュートリノによる Y_L, S 輸送の効果

流体不安定性

- 原始中性子星内部 (\sim neutrinosphere 内部) での不安定性

$$Y_L(r=0) \sim 0.3, Y_L(R_{\nu\text{sphere}}) \leq 0.1$$

$\Rightarrow dY_L/dr < 0$ lepton-driven convection (Y_L -driven)

dissipation of shock wave

$\Rightarrow dS/dr < 0$ entropy-driven convection (S-driven)



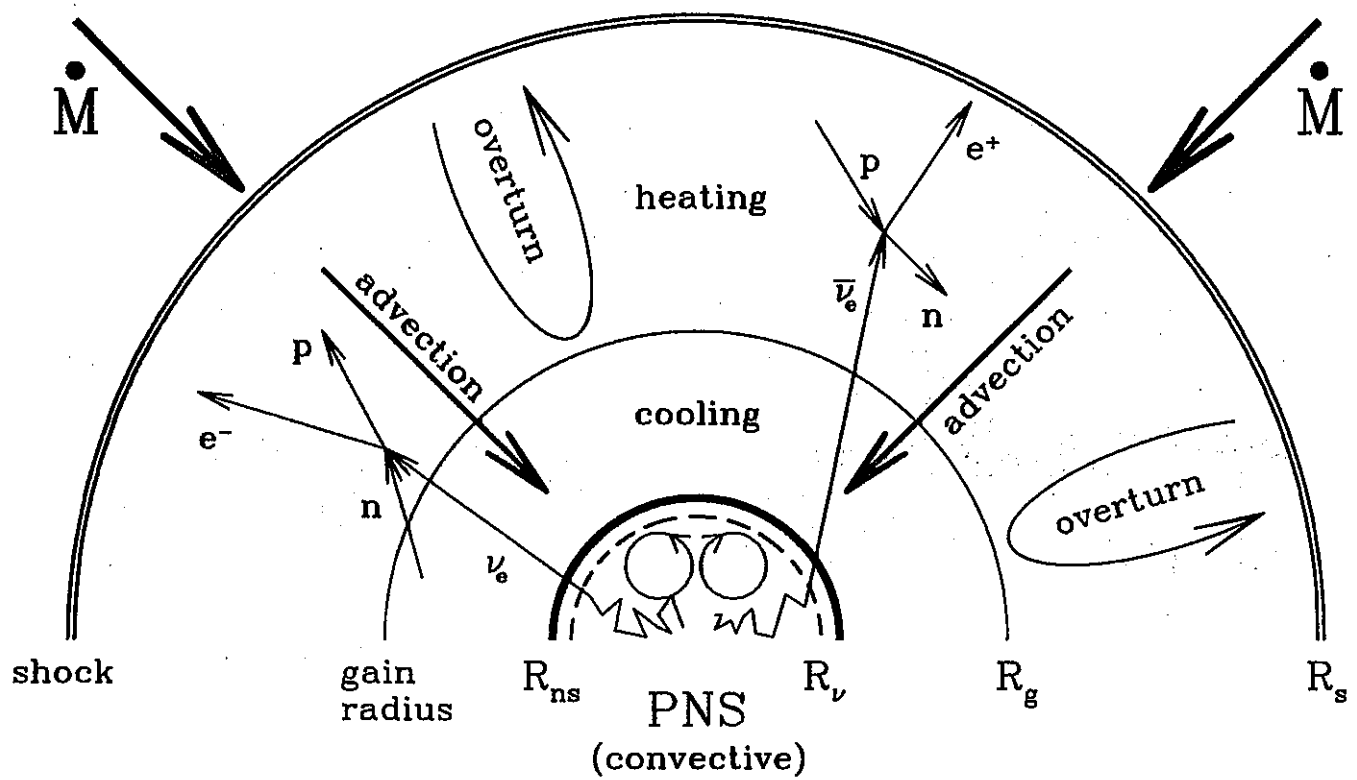
対流が原始中性子星内部の熱くレプトンを多く含んだ物質を表面 (\sim neutrinosphere) に運ぶ。

$\Rightarrow L_\nu \nearrow$, neutrino heating in the hot bubble \nearrow

定量的な影響: unclear/contradictory

- * Mayle and Wilson 1988, 1993
(1D with mixing length theory)
 $E_{\text{exp}}(\text{without convection}) < E_{\text{exp}}(\text{obs})$
convection is essential for the delayed explosion.
- * Burrows and Fryxell 1992 (2D without ν tr.)
vigorous S-driven convection
- * Burrows and Fryxell 1993 (2D with radial-ray ν tr.)
convectively enhanced $L_\nu \rightarrow$ explosion
- * Burrows, Hayes and Fryxell 1995
(2D with radial-ray ν tr.)
S-/ Y_L -driven convection: weak and unimportant
- * Herant *et al.* 1994
(2D SPH + EIFLD/central light bulb ν tr.)
intermittent Y_L -driven convection
- * Keil, Janka and Müller 1996
(2D with radial-ray ν transfer)
 Y_L -driven convection evolves (whole PNS)
 $L_\nu \nearrow$ factor 2, $\langle \omega_\nu \rangle \nearrow$ factor 1.1-1.2
- * Bruenn and Mezzacappa 1994 (1D mixing length theory + MGFLD)

Tanka



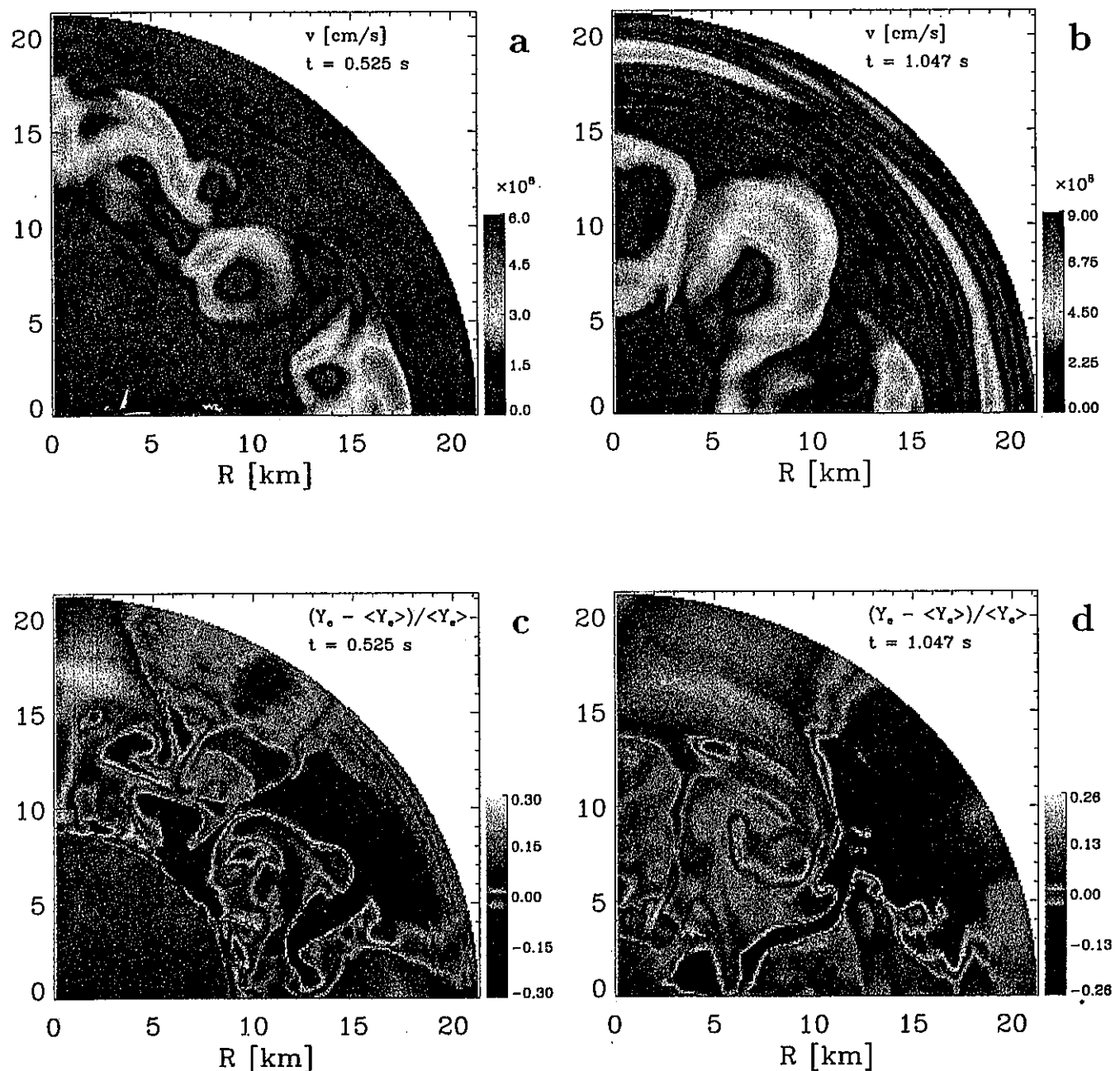


Figure 3:

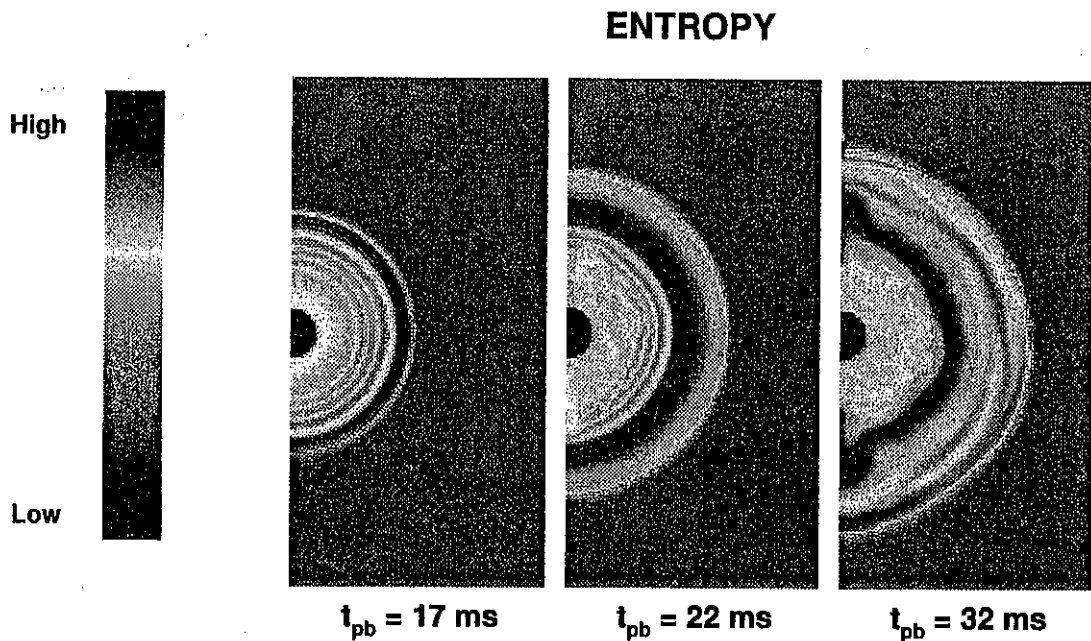


Fig. 10a.— Two-dimensional plots showing the entropy evolution of the $15 M_\odot$ model in a simulation without neutrino transport (simulation K).

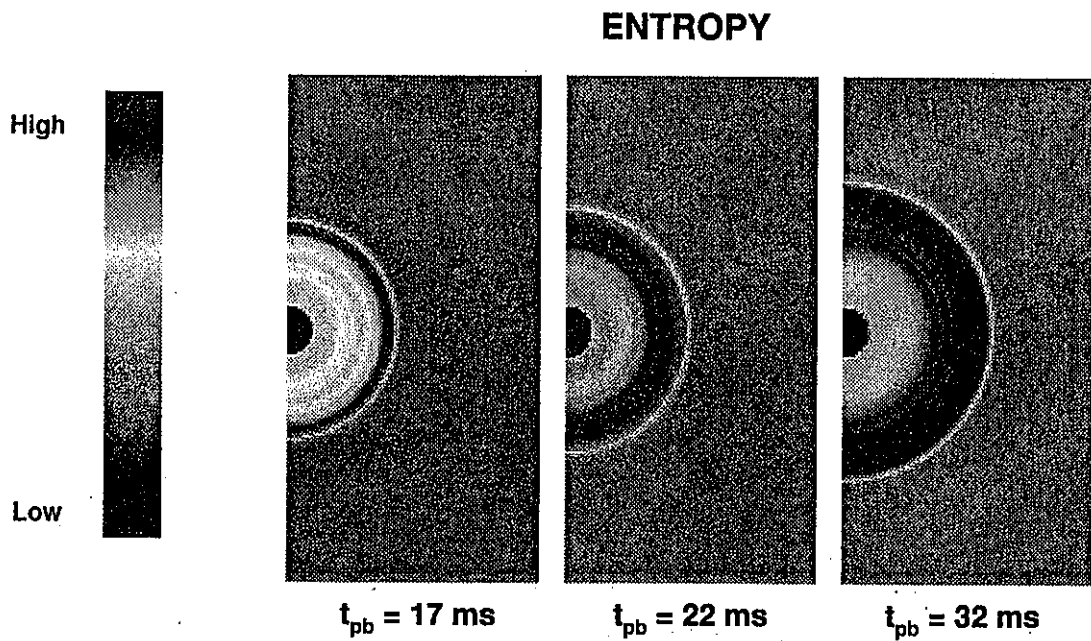


Fig. 11a.— Two-dimensional plots showing the entropy evolution of the $15 M_\odot$ model in a simulation with neutrino transport (simulation L).

- 衝撃波と neutrinosphere 間における不安定性

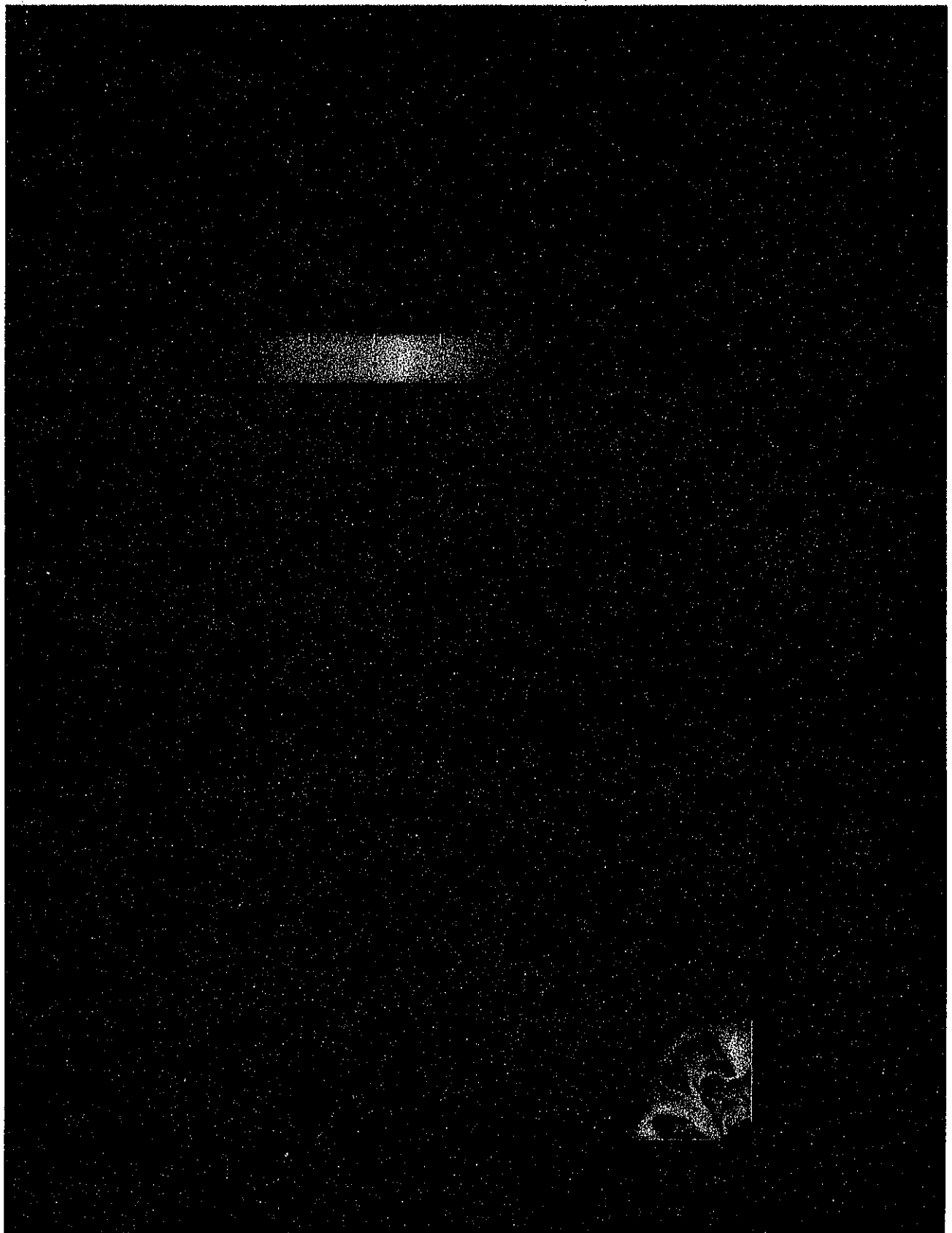
gain radius: 実質的なニュートリノ加熱率(ニュートリノ加熱 - ニュートリノ冷却)が最大となるところ

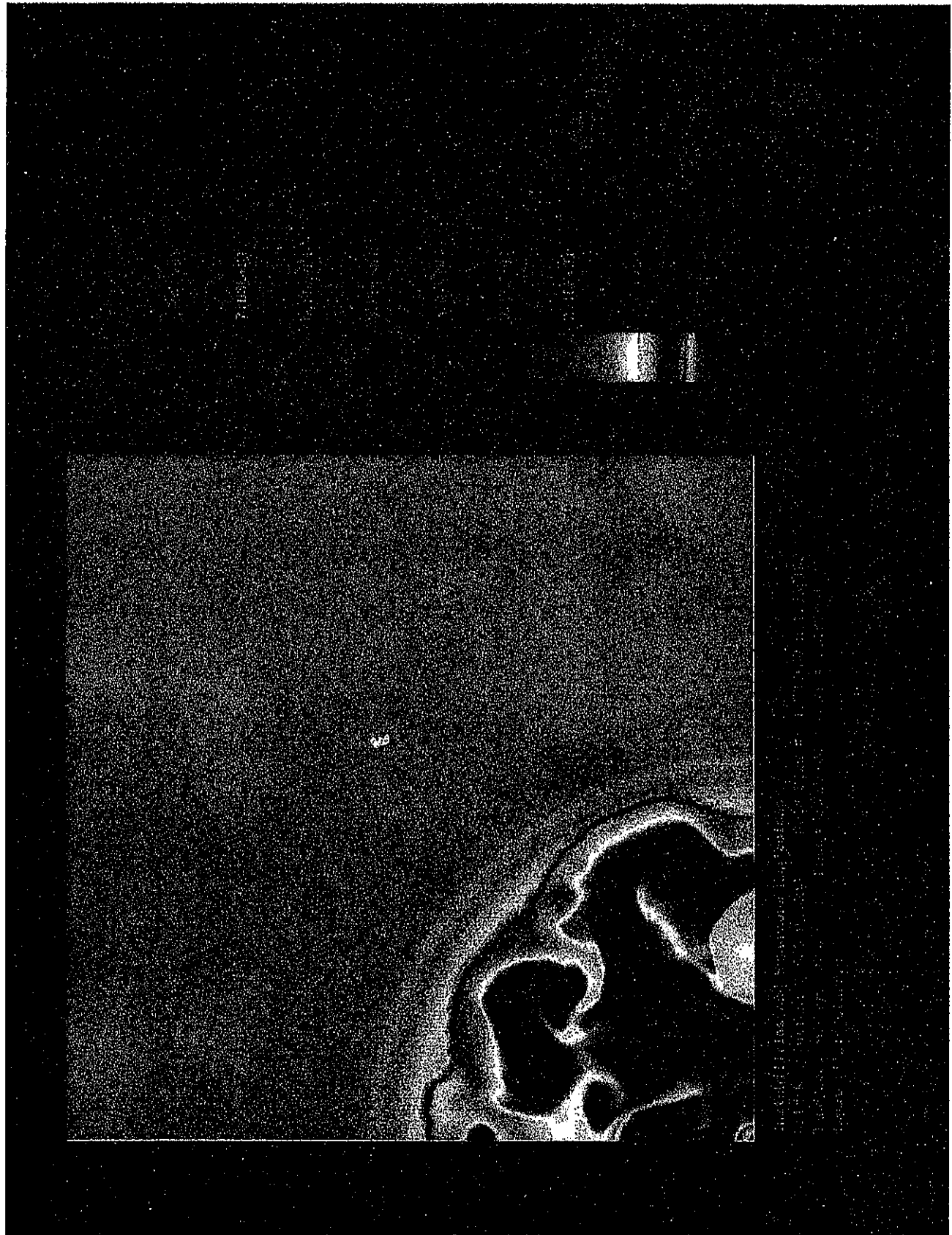
1. 超音速で落下する物質(原子核)
2. 衝撃波面を通過($A \rightarrow np$)
3. ゆっくりと落下: $R_{\text{shock}} > r > R_{\text{gain}}$
($\nu_e n \rightarrow e^- p, \bar{\nu}_e p \rightarrow e^+ n$ による加熱)
4. gain radius を通過: $r < R_{\text{gain}}$
(ニュートリノ放出により冷却)
5. 原始中性子星の上に降着
重力エネルギー \Rightarrow ニュートリノ放出

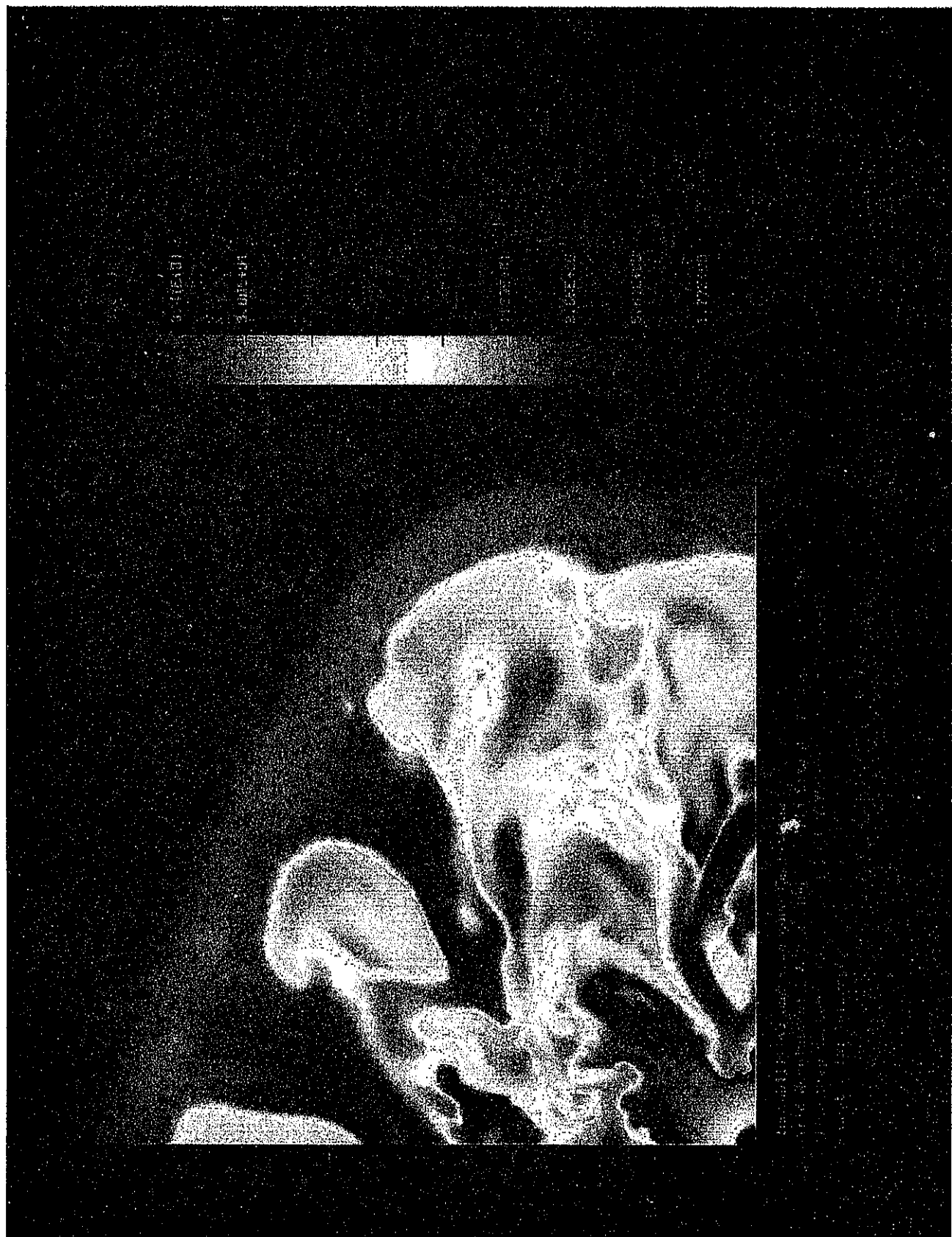
$dS/dr(R_{\text{gain}} < r < R_{\text{shock}}) < 0$: S-driven convection
= ν -driven convection

対流が、 R_{gain} で暖められた物質を、ニュートリノ放出 ($\propto T^6, T^9$) によって冷えてしまう前に衝撃波面へ運ぶ。

- * Herant *et al.* 1992–1994
(2D SPH + EIFLD/central light bulb ν tr.)
large scale flow \rightarrow robust explosion
high S matter: $R_{\text{gain}} \rightarrow R_{\text{shock}}$
low S matter: $R_{\text{shock}} \rightarrow R_{\text{gain}}$
- * Miller, Wilson and Mayle 1993
(2D + 2D EIFLD ν tr.)
large scale flow, not help the explosion
- * Burrows, Hayes and Fryxell 1995
(2D + radial-ray ν tr.)
turbulent flow \rightarrow some models explode (not robust)
 $S(2D) > S(1D)$, pressure of buoyant plume
 $\rightarrow R_{\text{shock}}(2D) > R_{\text{shock}}(1D)$
 \rightarrow gravitational potential \searrow , accretion ram \searrow
 \rightarrow explosion
- * Janka and Müller 1995, 1996
(1D/2D + radial-ray ν tr.)







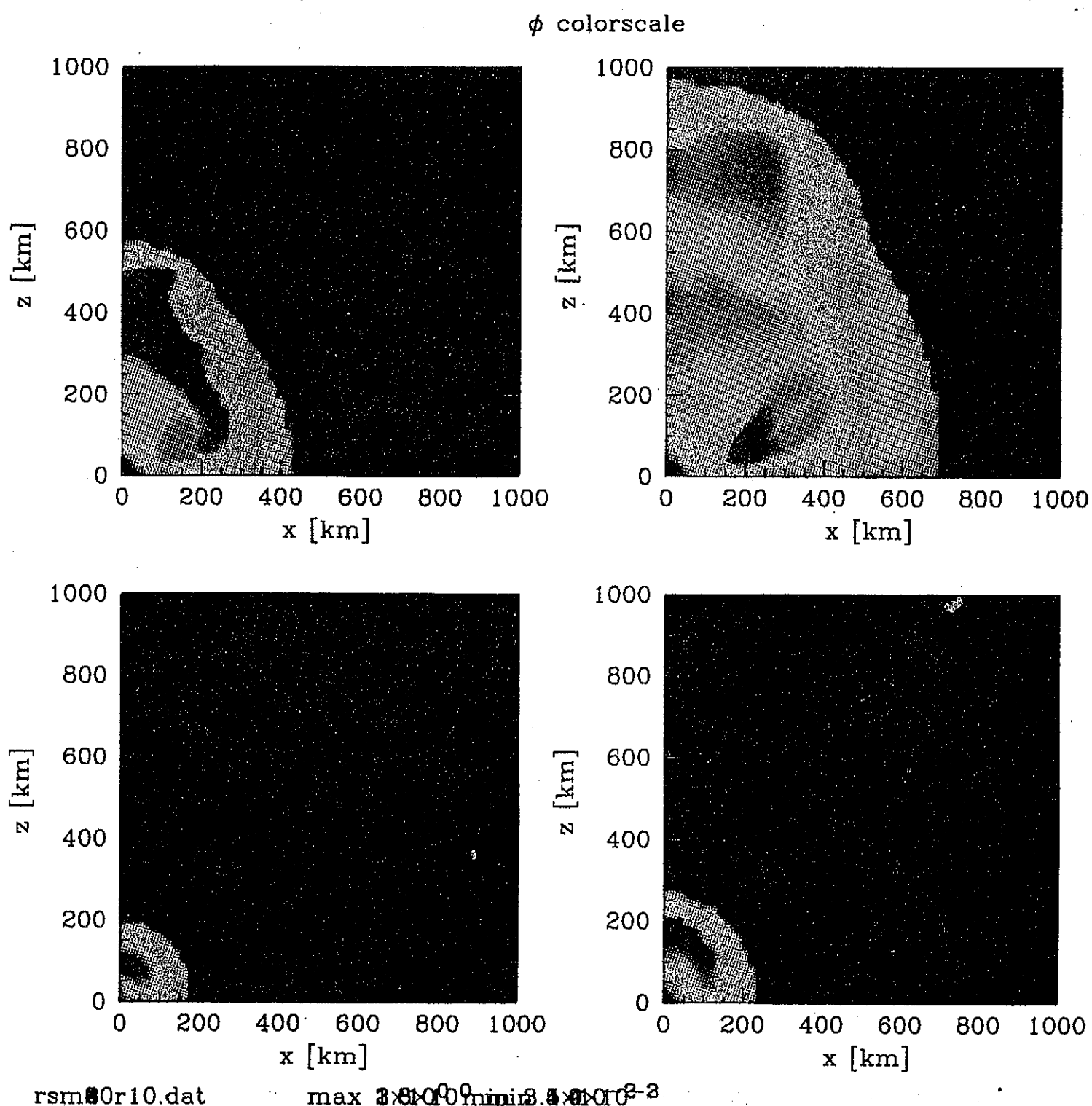
回転?

Shimizu *et al.* 1994: asymmetric neutrino emission from the rotating protoneutron star

→ jet-like explosion E_{shock} ↗

Shimizu et al.

エントロピー分布



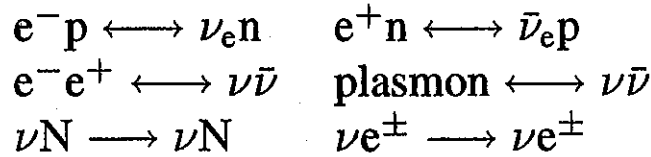
- 原始中性子星の冷却 $\tau \sim \tau_{\text{diff}} = O(10)\text{sec}$

$\tau_{\text{dyn}} \sim 1\text{msec} \ll \tau_{\text{diff}}$: 準静的進化

hot lepton-rich PNS	ν 's diffuse out	cold Neutron Star
$T \sim O(10)\text{MeV}$		$T \sim 0$
$\mu_{\nu_e} \sim O(100)\text{MeV}$		$\mu_p + \mu_e - \mu_n \sim 0$ (ν -less β -equilibrium)
$R \sim 100\text{km}$		$R \sim 10\text{km}$

$$\begin{aligned} \lambda_\nu (\rho = 10^{14}\text{g/cm}^3) &= 1/\sigma_{\text{weak}} n_{\text{baryon}} \\ 10^3 \text{cm} \left(\frac{\omega_\nu}{10\text{MeV}} \right)^{-2} &= 10^7 \text{cm} \left(\frac{\omega_\nu}{100\text{keV}} \right)^{-2} \end{aligned}$$

$$\sigma_{\text{weak}} \sim \frac{4G_F^2 \hbar^2 c^2}{\pi} \omega_\nu^2$$



冷たく中性子の割合が多い(陽電子・陽子が少ない)領域では、
核子制動輻射: $NN' \longleftrightarrow NN' \nu \bar{\nu}$ が重要となる。

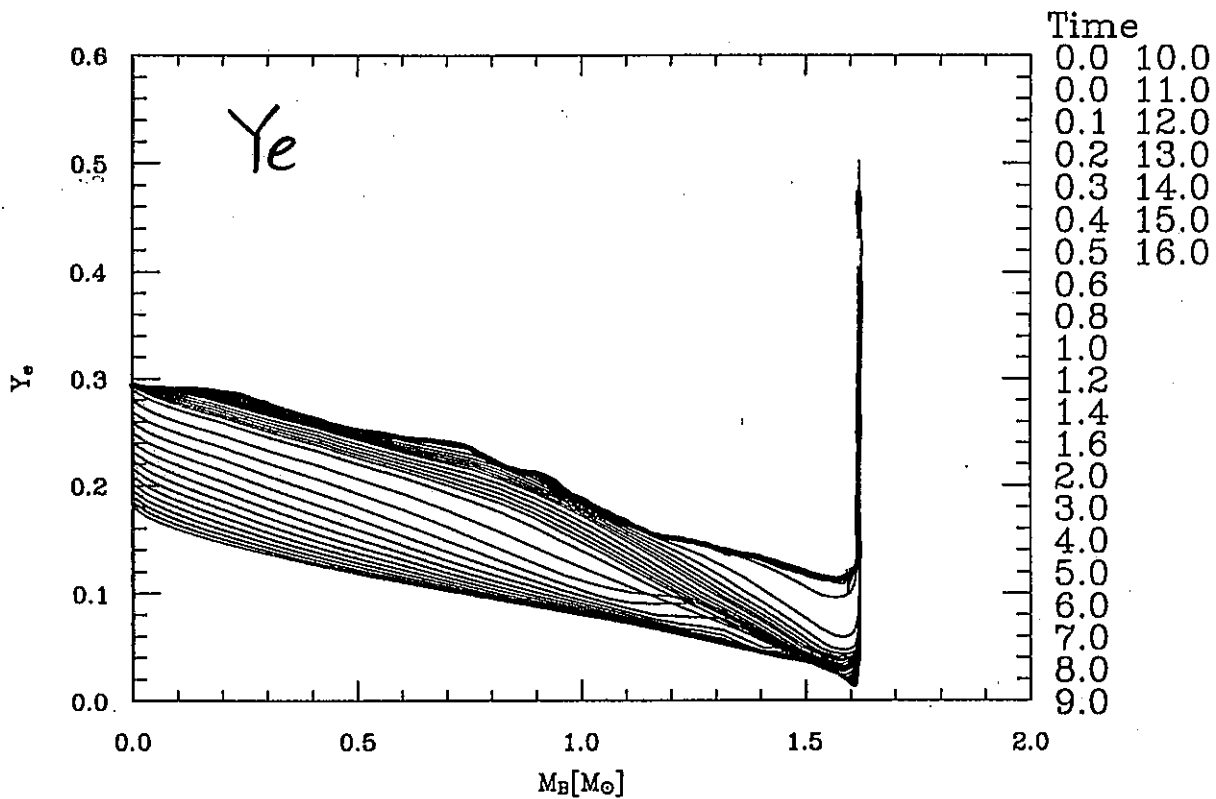
- 星の爆発(超新星爆発)

コアの爆発後、星の外層を衝撃波が伝播

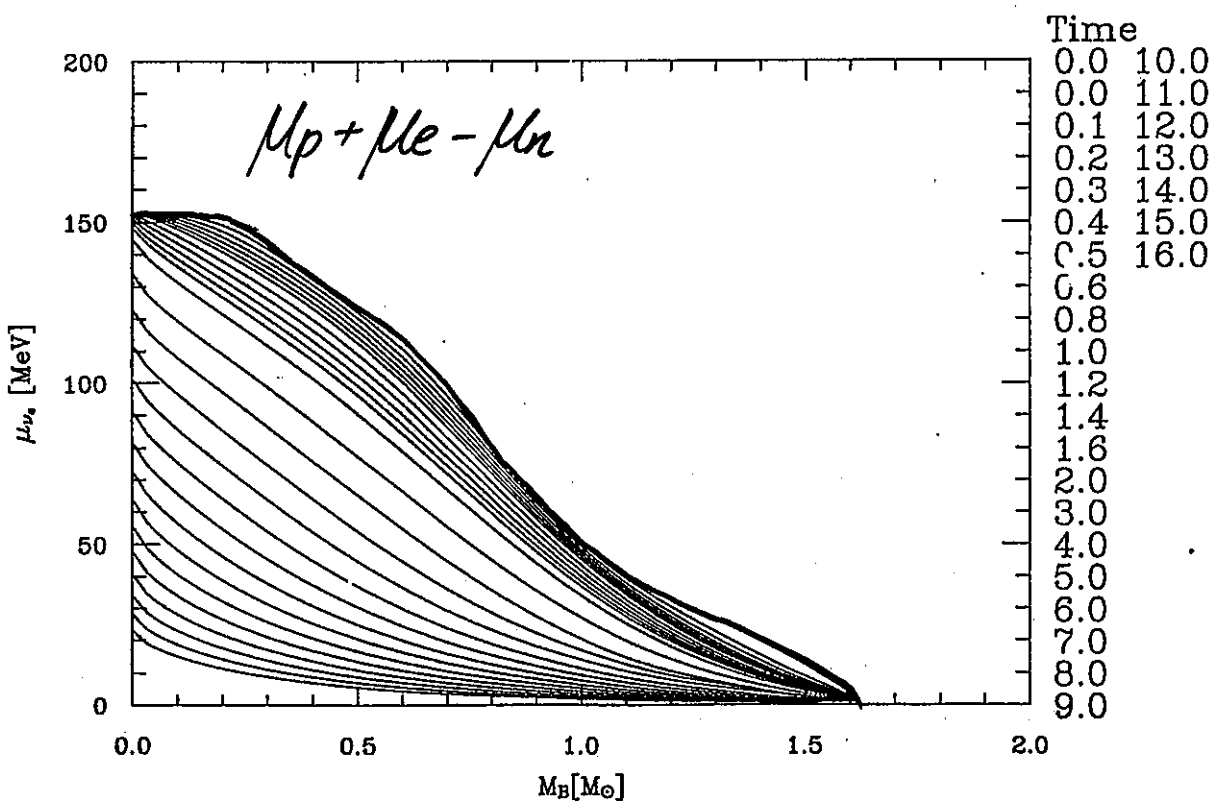
↓ 光分解、ニュートリノ放出: negligible
 $E_{\text{bind}}(\text{envelope}) \ll 10^{51}\text{erg}$

successful explosion (supernova explosion): $\tau = \text{hours} \sim \text{days}$

MW88C48

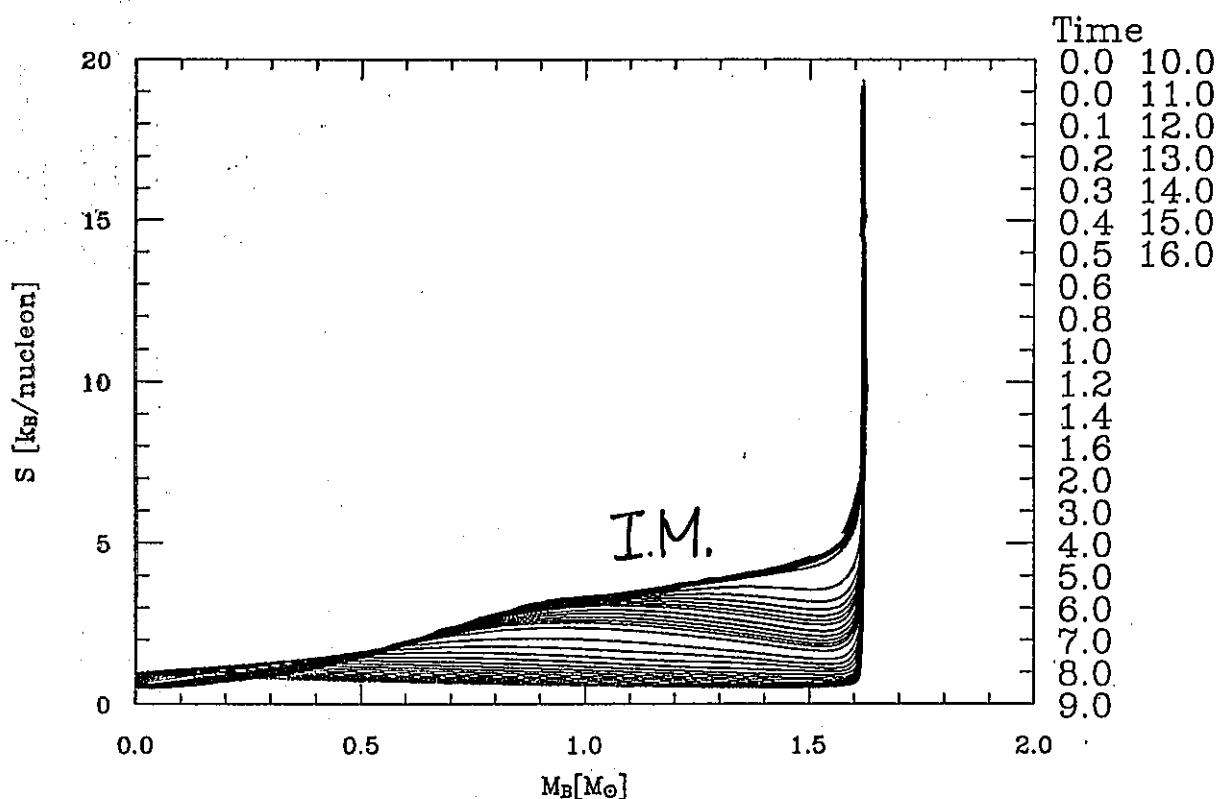


MW88C48



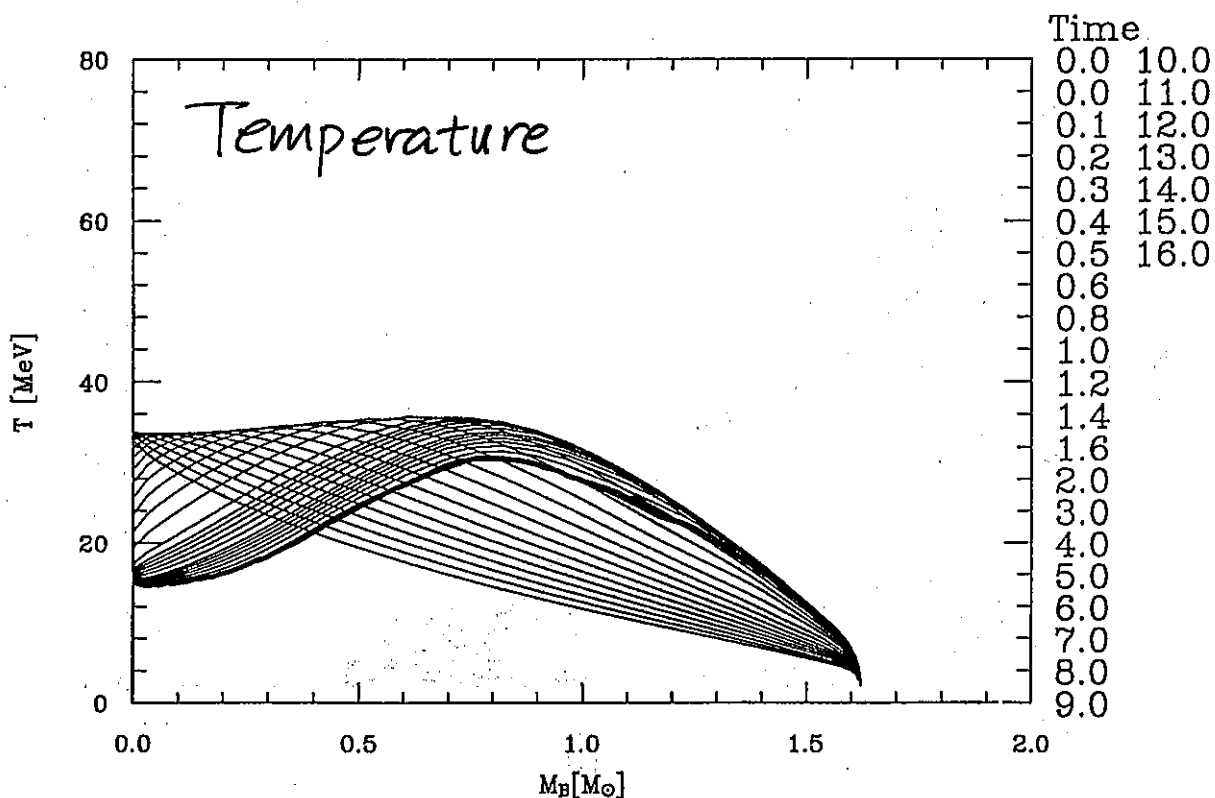
Entropy

MW88C48



↓ rapid cooling of outer core $S \downarrow T \uparrow (P \uparrow)$
 heating of inner core
 cooling of whole PNS.

MW88C48



2 超新星ニュートリノ

Energetics

$$\Delta E_G = \left(\frac{GM_{\text{core}}^2}{R_{\text{Fe core}}} - \frac{GM_{\text{core}}^2}{R_{\text{NS}}} \right) \sim O(10^{53}) \text{erg}$$

$$E_{\text{kin}} \sim O(10^{51}) \text{erg} \quad (\text{obs.})$$

$$E_{\text{rad}} \sim O(10^{49}) \text{erg} \quad (\text{obs.})$$

$$E_{GW} \sim O(10^{51}) \text{erg} \quad (\text{simulations(slow rot.) by Stark \& Piran})$$

残り $O(10^{53}) \text{erg} \sim E_\nu$ cf. $E_\nu(\text{SNIa}) < 10^{49} \text{erg}$

すべての陽子が中性子に变成了としても放出される ν_e は、

$$26 \frac{M_{\text{Fe core}}}{m_{\text{Fe}}} \langle E_{\nu_e} \rangle \sim 1.2 \cdot 10^{52} \text{erg} \frac{M_{\text{Fe core}}}{1.4 M_\odot} \frac{\langle E_{\nu_e} \rangle}{10 \text{MeV}}$$

であり $E_{\nu \text{ tot}} \sim O(10^{53}) \text{erg}$ の 10% でしかない。

\Rightarrow thermal $\nu \gg$ 電子捕獲に伴う ν_e

$\Rightarrow \nu_e, \bar{\nu}_e, \nu_\mu$ がほぼ同等に寄与

$$E_{\nu_e}(\text{collapse}) \sim 10^{51} \text{erg}$$

$$E_{\nu_e}(\text{neutronization burst}) \sim 10^{51} \text{erg}$$

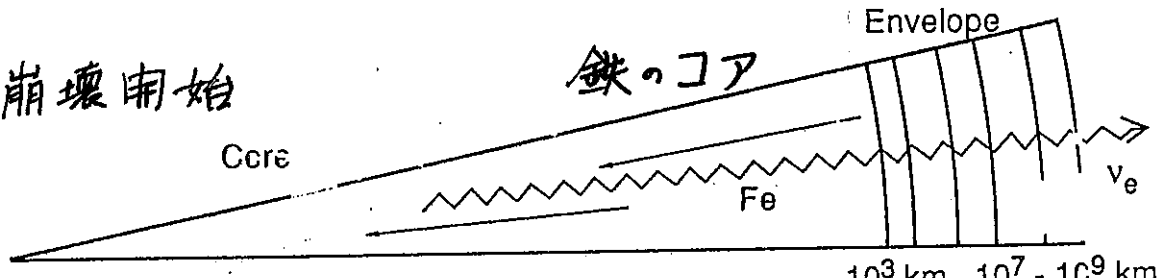
$$E_\nu(\text{shocked accreted matter}) \sim 10^{53} \text{erg}$$

$$E_\nu(\text{PNScooling}) \sim 10^{53} \text{erg}$$

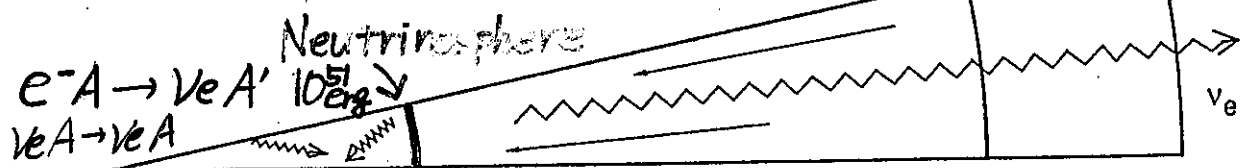
平均エネルギー

$$\begin{array}{ccl} \sigma_{\nu_e} & > & \sigma_{\bar{\nu}_e} \\ R(\nu_e \text{sphere}) & > & R(\bar{\nu}_e \text{sphere}) \\ T(\nu_e \text{sphere}) & < & T(\bar{\nu}_e \text{sphere}) \\ \langle \omega_{\nu_e} \rangle & < & \langle \omega_{\bar{\nu}_e} \rangle \end{array} \quad \begin{array}{ccc} & & \sigma_{\nu_\mu} \\ & & > \\ & & R(\nu_\mu \text{sphere}) \\ & & < \\ & & \langle \omega_{\nu_\mu} \rangle \end{array}$$

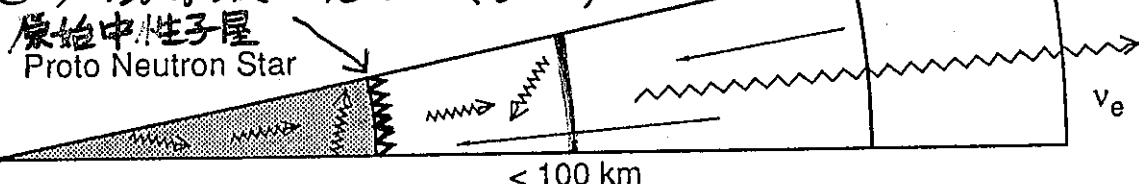
重力崩壊開始



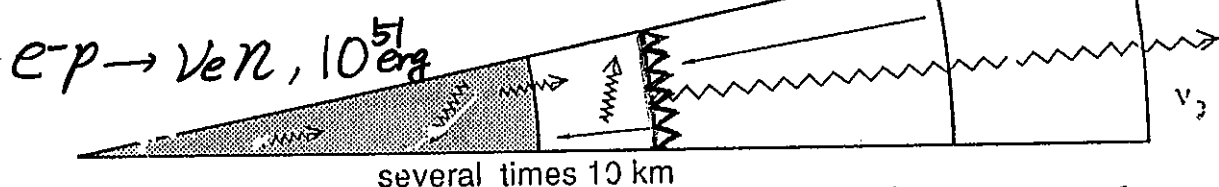
ニュートリノの漏洩



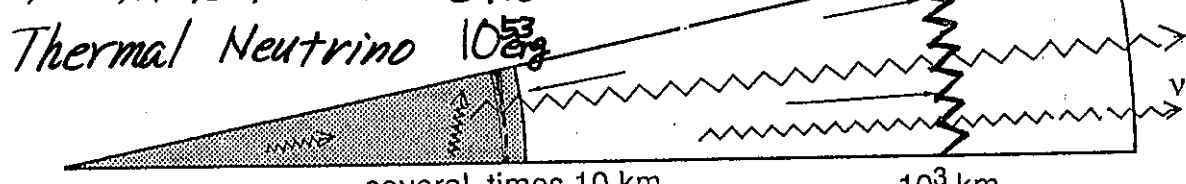
Bounce, 衝撃波の発生 ($t=0$)



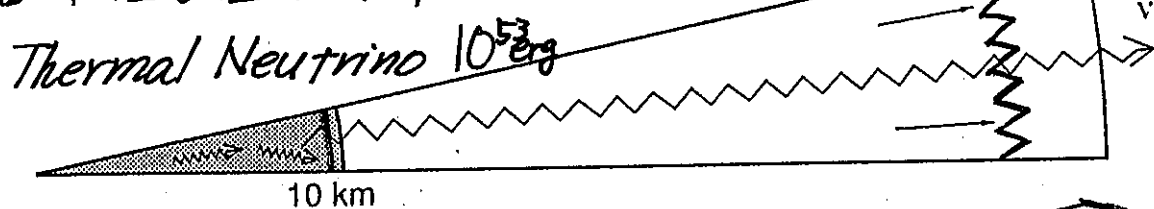
中性子化バースト ($t \sim 10 \text{ msec}$)



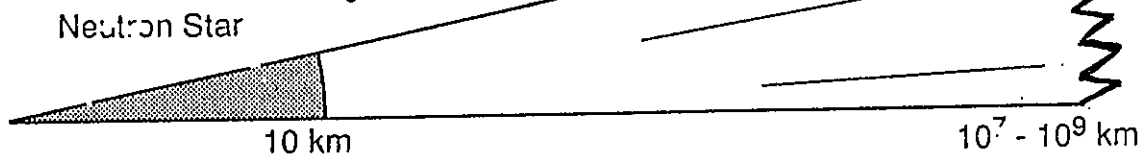
コアの爆発, Accretion ($t = 10 \text{ ms} \sim 1 \text{ s}$)

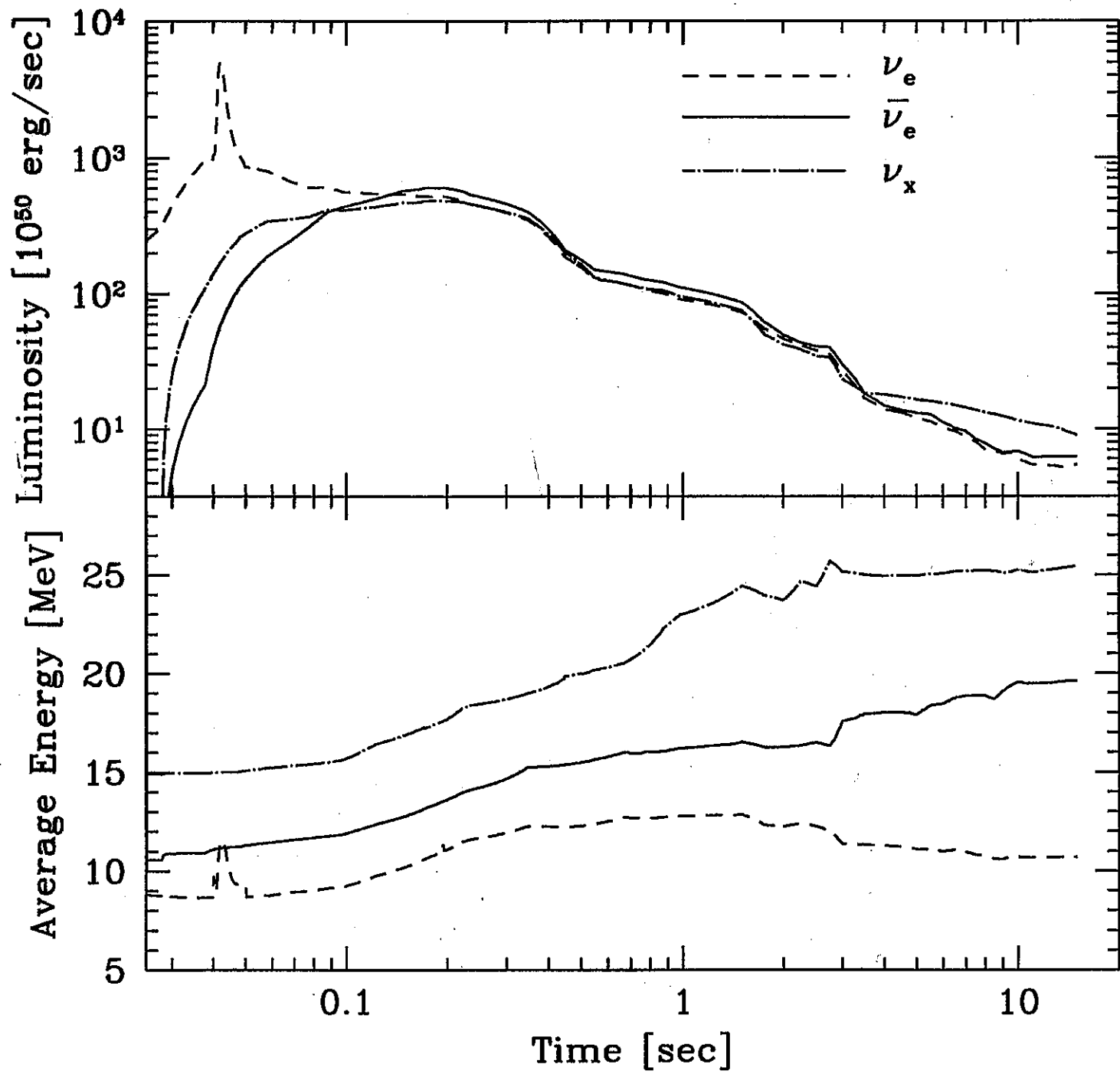


原始中性子星の冷却 ($t = 1 \sim 10 \text{ s}$)



超新星爆発 10^{51} erg $t >$ 数時間





Wilson

$M \sim 20M_{\odot}$

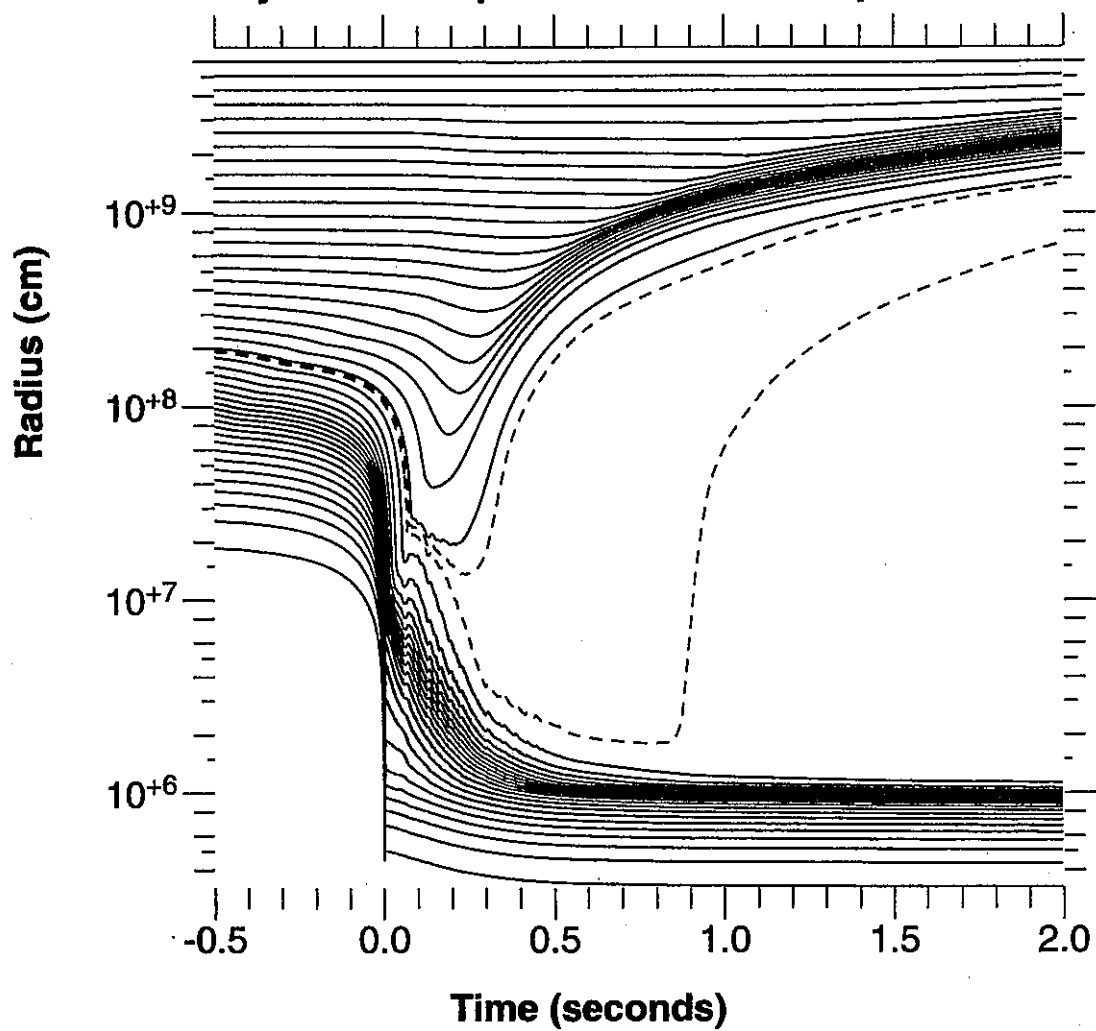
$$\int L dt = 2.9 \cdot 10^{53} \text{ erg}$$

$$\int \bar{\nu}_e dt = 4.7 \cdot 10^{52} \text{ erg}, \langle W \bar{\nu}_e \rangle = 15.3 \text{ MeV}$$

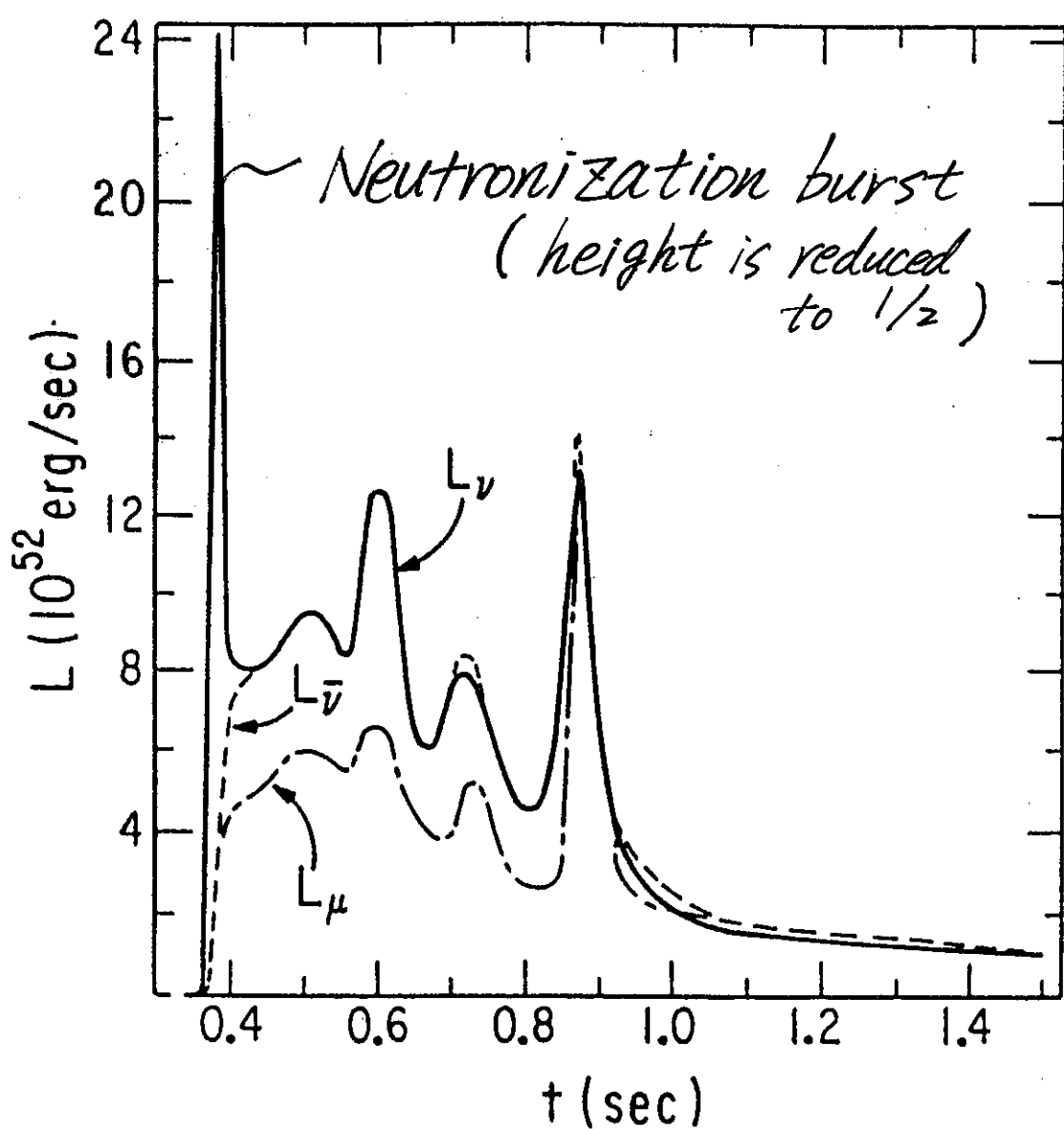
Totani et al. '98

Mass trajectory points versus time

Solid: every fifth mass point Dashed: mass points 108 and 109



Supernova Vs



Mayle Wilson Schramm
delayed explosion

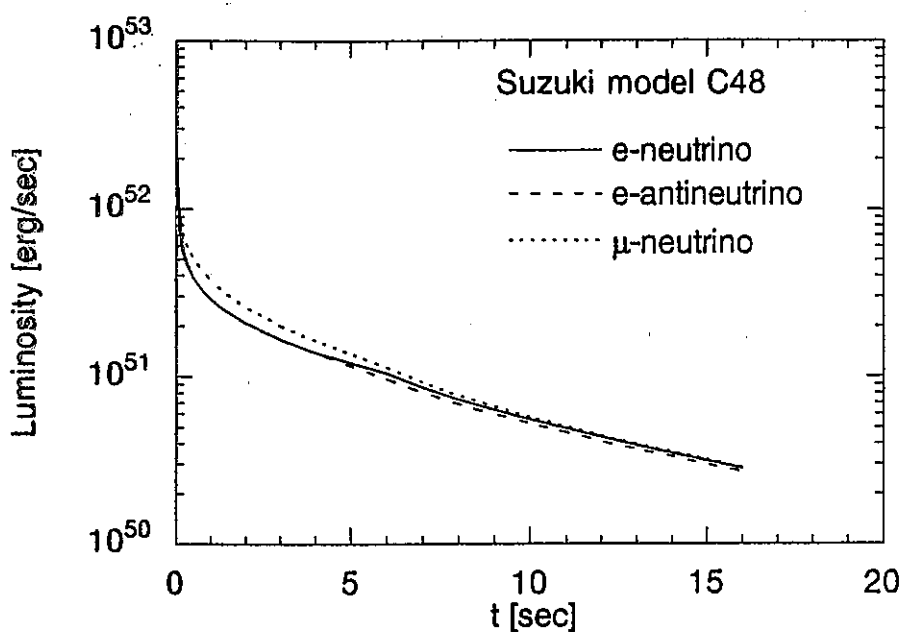


Figure 28: Evolution of the neutrino luminosity at the cooling stage of the protoneutron star (Suzuki: model C48 [113]). Solid line is ν_e 's, dashed is $\bar{\nu}_e$'s and dot-dashed is ν_μ 's, respectively

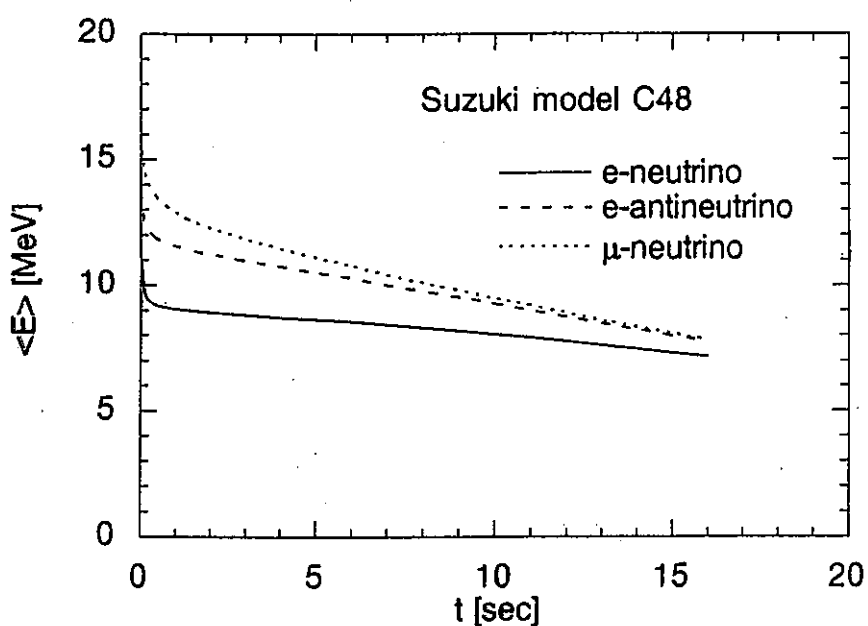


Figure 29: Mean energy of neutrino burst at the cooling stage of the protoneutron star (Suzuki: model C48 [113]). Solid line is ν_e 's, dashed is $\bar{\nu}_e$'s and dot-dashed is ν_μ 's, respectively

ニュートリノのエネルギースペクトル

$\neq R_\nu$ からの黒体輻射 ($\mu_\nu = 0$ の Fermi-Dirac) スペクトル

$\sim R_\nu(E)$ からの β -平衡 Fermi-Dirac スペクトルの重ね合わせや、 $R_{th}(E)$ からの熱平衡 Fermi-Dirac スペクトルに散乱による抑制因子をかけて重ね合わせたもの

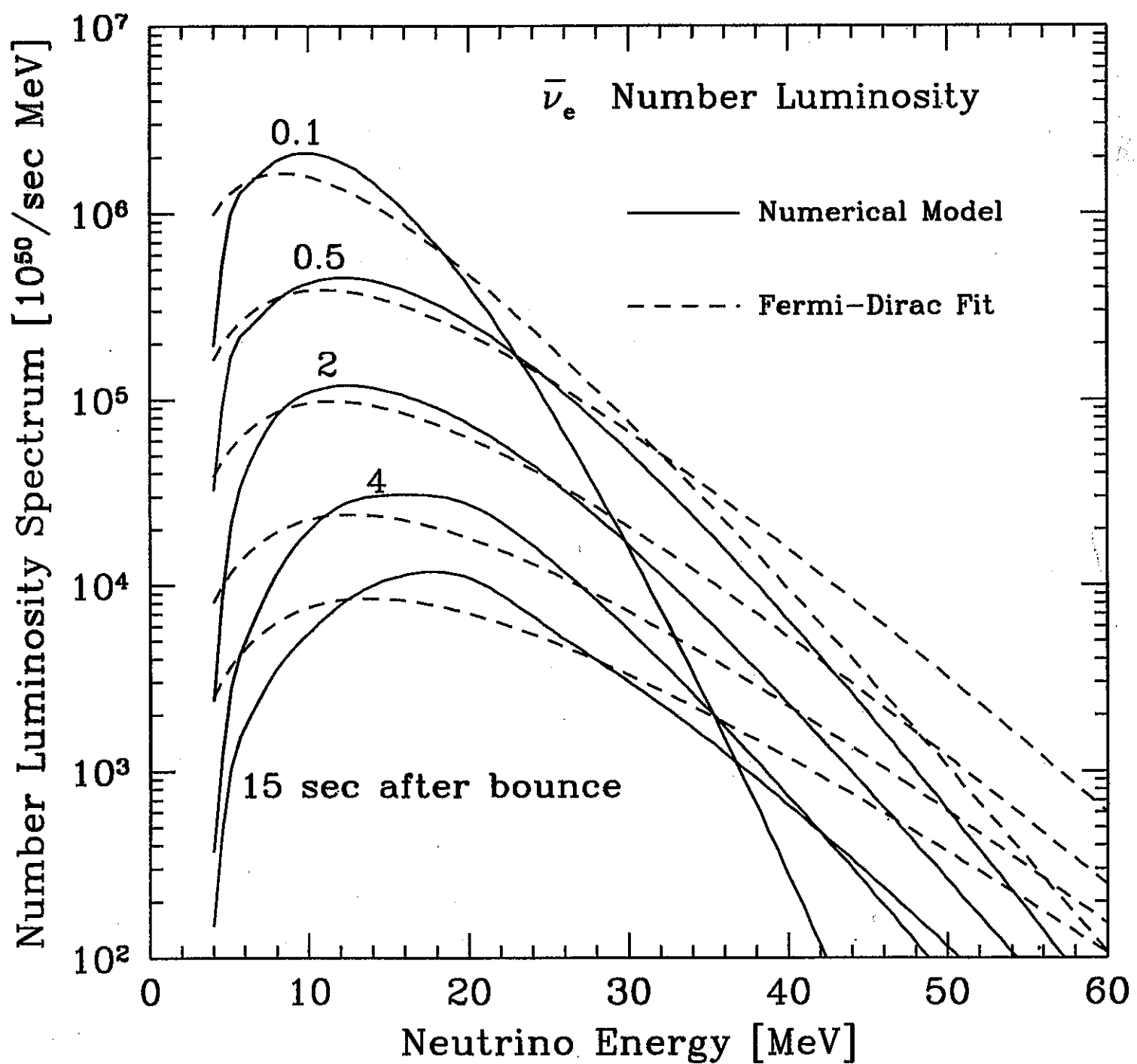
Fermi-Dirac スペクトルによる fitting

$$\begin{aligned} L_\nu &= \frac{c}{4} 4\pi R^2 \frac{4\pi}{(hc)^3} \int \frac{E_\nu^3 dE_\nu}{e^{(E_\nu - \mu)/T} + 1} \\ &= \frac{c}{4} 4\pi R^2 \frac{4\pi}{(hc)^3} T^4 F_3(\eta) \end{aligned}$$

$$\begin{aligned} \langle E_\nu \rangle &= L_\nu \Big/ \frac{c}{4} 4\pi R^2 \frac{4\pi}{(hc)^3} \int \frac{E_\nu^2 dE_\nu}{e^{(E_\nu - \mu)/T} + 1} \\ &= T F_3(\eta) / F_2(\eta) \end{aligned}$$

$$\begin{aligned} \langle E_\nu^2 \rangle / \langle E_\nu \rangle^2 &= \int \frac{E_\nu^4 dE_\nu}{e^{(E_\nu - \mu)/T} + 1} \Big/ \int \frac{E_\nu^2 dE_\nu}{e^{(E_\nu - \mu)/T} + 1} \langle E_\nu \rangle^2 \\ &= F_4(\eta) F_2(\eta) / F_3(\eta)^2 \end{aligned}$$

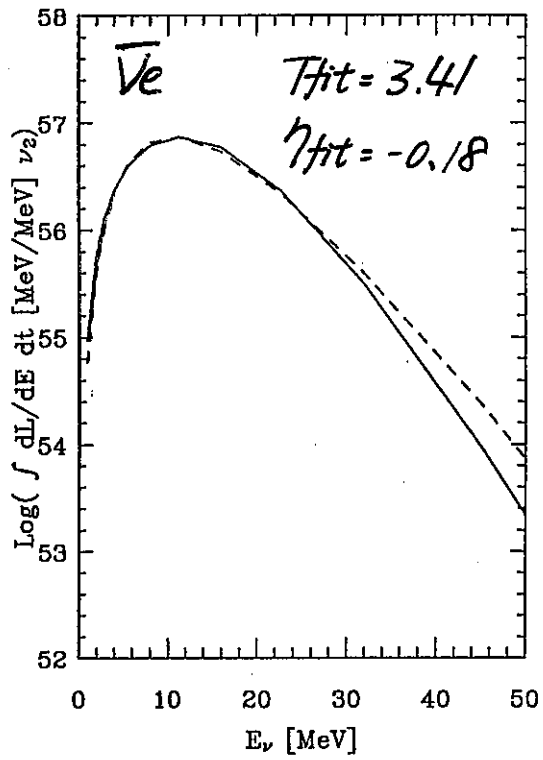
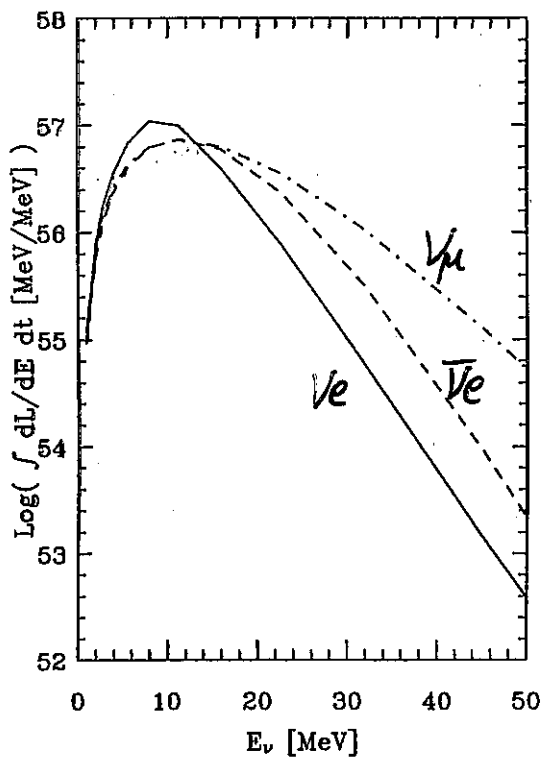
$$F_n(\eta) \equiv \int_0^\infty \frac{x^n dx}{e^{x-\eta} + 1}$$



Time Integrated Energy Spectrum

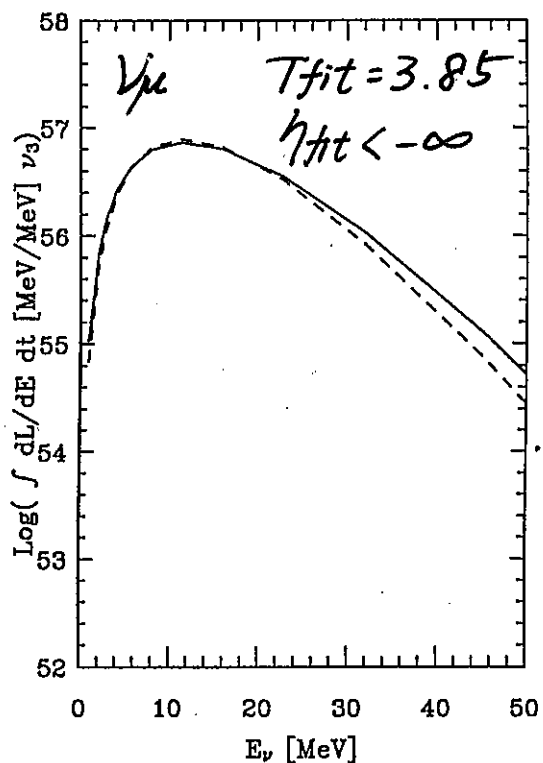
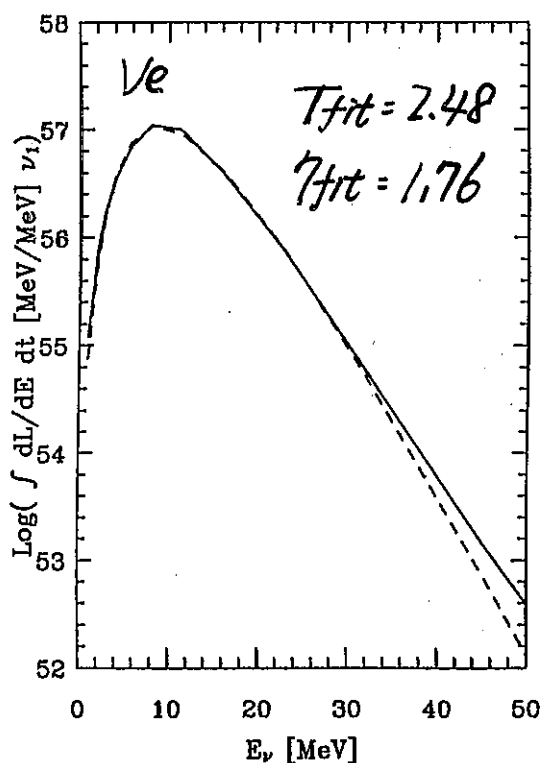
MW88C48 t = 16.0

MW88C48 t = 16.0



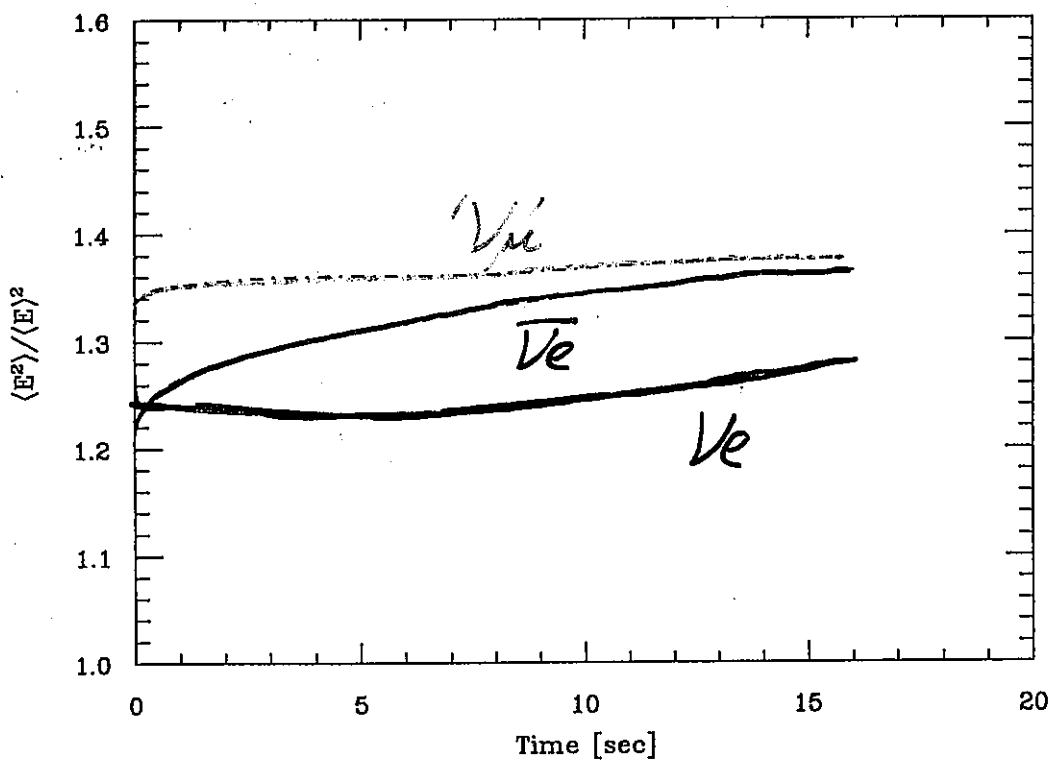
MW88C48 t = 16.0

MW88C48 t = 16.0

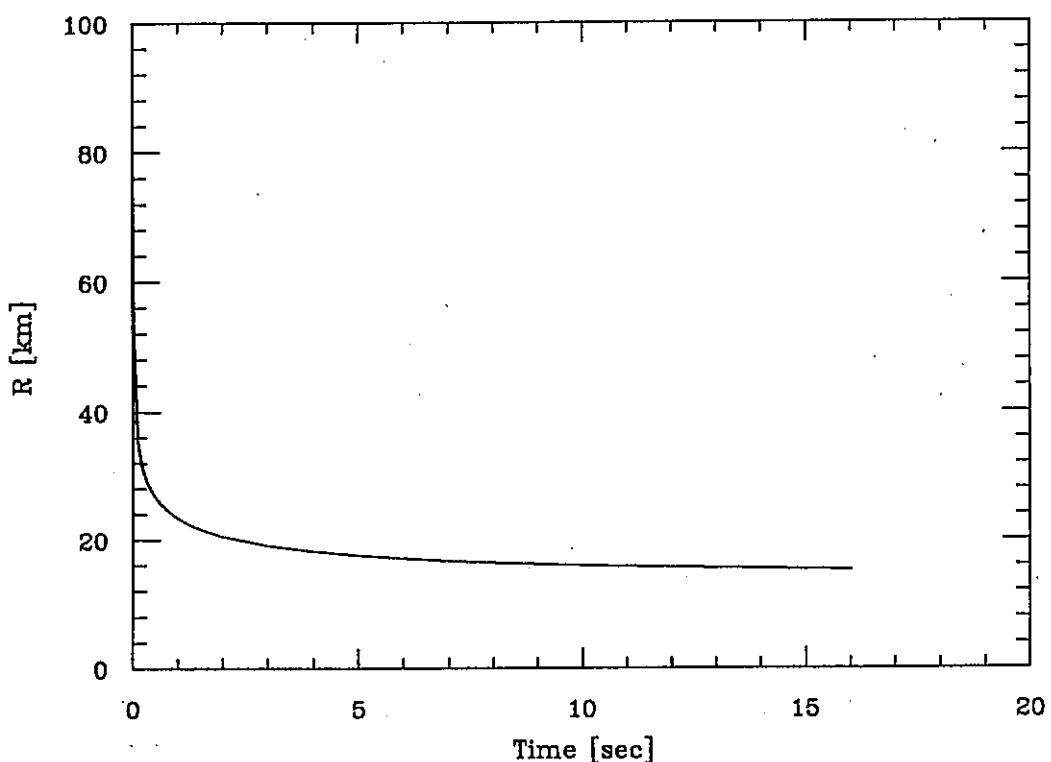


peak width of emergent V flux

MW88C48



MW88C48



入力物理の影響

* prompt explosion

$$\begin{aligned}
 E_{\text{shock}} &\sim \frac{GM_{\text{i.c.}}^2}{R_{\text{i.c.}}} \propto M_{\text{i.c.}}^{5/3} \rho_c^{1/3} \propto Y_{L\text{trap}}^{10/3} \rho_c^{1/3} \\
 E_{\text{dissociation}} &\sim \frac{30m_n + 26m_p - m_{\text{Fe}}}{m_{\text{Fe}}} (M_{\text{Fe core}} - M_{\text{i.c.}}) c^2 \\
 &= 8 \cdot 10^{51} \text{erg} \frac{M_{\text{Fe core}} - M_{\text{i.c.}}}{0.5M_\odot} \\
 M_{\text{i.c.}} &\propto Y_{L\text{trap}}^2
 \end{aligned}$$

- Soft EOS is better
(Takahara and Sato, Baron *et al*, Bruenn)

$$\begin{aligned}
 \text{small adiabatic index } \gamma &= \frac{\partial \ln P}{\partial \ln \rho} \\
 \text{small imcompressibility } K_0 &= 9 \left. \frac{\partial P}{\partial \rho} \right|_{\rho_{\text{nuc}}} \Rightarrow \text{high } \rho_c \Rightarrow E_{\text{shock}} \nearrow
 \end{aligned}$$

$M = 1.4M_\odot$ の NS の存在 \rightarrow Soft 過ぎてもダメ

- 電子捕獲率 at $\rho < \rho_{\text{trap}} \sim 10^{12} \text{g/cm}^3$
($\nu_e \text{escape} \Rightarrow Y_{L\text{trap}} \searrow$)
shell blocking \Rightarrow e-cap rate $\searrow \Rightarrow Y_{L\text{trap}} \nearrow \Rightarrow E_{\text{shock}} \nearrow$
Bruenn 1985: $N \geq 40$ p($f_{7/2}$) \rightarrow n($f_{5/2}$) is blocked.
- 自由陽子の存在量 at $\rho < \rho_{\text{trap}}$
 $\sigma_{e\text{-cap}}(p) > \sigma_{e\text{-cap}}(A)$
 $X_p \searrow \Rightarrow$ e-cap rate $\searrow \Rightarrow Y_{L\text{trap}} \nearrow \Rightarrow E_{\text{shock}} \nearrow$
- neutrino opacity at $\rho < \rho_{\text{trap}}$
neutrino opacity $\nearrow \Rightarrow Y_{L\text{trap}} \nearrow \Rightarrow E_{\text{shock}} \nearrow$
down scattering (νe^- (degenerate) $\rightarrow \nu e^-$, $\nu A \rightarrow \nu A^*$)

$$\begin{aligned}
 \omega_\nu \searrow &\Rightarrow \text{neutrino opacity } \searrow \\
 S \nearrow &\Rightarrow X_p \nearrow \Big) \Rightarrow E_{\text{shock}} \searrow
 \end{aligned}$$

Iron core mass

Table I
"Iron core" masses (M_{\odot})

Weaver & Woosley '93

Model ^a	$12 M_{\odot}$	$13 M_{\odot}$	$15 M_{\odot}$	$20 M_{\odot}$	$25 M_{\odot}$	$30 M_{\odot}$	$35 M_{\odot}$	$40 M_{\odot}$
0.5 S	-	-	1.49	-	1.49	-	1.78	-
1.0 S	-	-	1.41	-	1.47	-	1.48	-
1.5 S	1.45	1.44	1.64	1.48	1.62	1.73	1.74	1.88
1.7 S	1.43	1.45	1.52	1.53	1.60	1.86	1.94	1.78
2.0 S	1.37	1.55	1.39	1.74	1.97	2.05	2.05	2.15
3.0 S	-	-	1.41	-	1.52	-	1.93	-
0.5 N	-	-	1.42	-	1.44	-	1.60	-
1.0 N	-	-	1.35	-	1.38	-	1.65	-
1.5 N	-	-	1.37	-	1.43	-	1.64	-
1.7 N	-	-	1.25	1.40	1.47	1.70	1.57	1.78
2.0 N	-	-	1.23	1.72	1.52	1.73	1.74	1.95
3.0 N	-	-	1.41	-	1.61	-	2.05	-

^aThe number labeling each row gives the multiplier used for the $^{12}\text{C}(\alpha, \gamma)^{16}\text{O}$ rate (relative to the value of Caughlan and Fowler [1988]); the letter "S" indicates a model with nominal semiconvection, while the letter "N" indicates a model with restricted semiconvection.

1.20 1.28 1.40 1.61 Nomoto Hashimoto '88

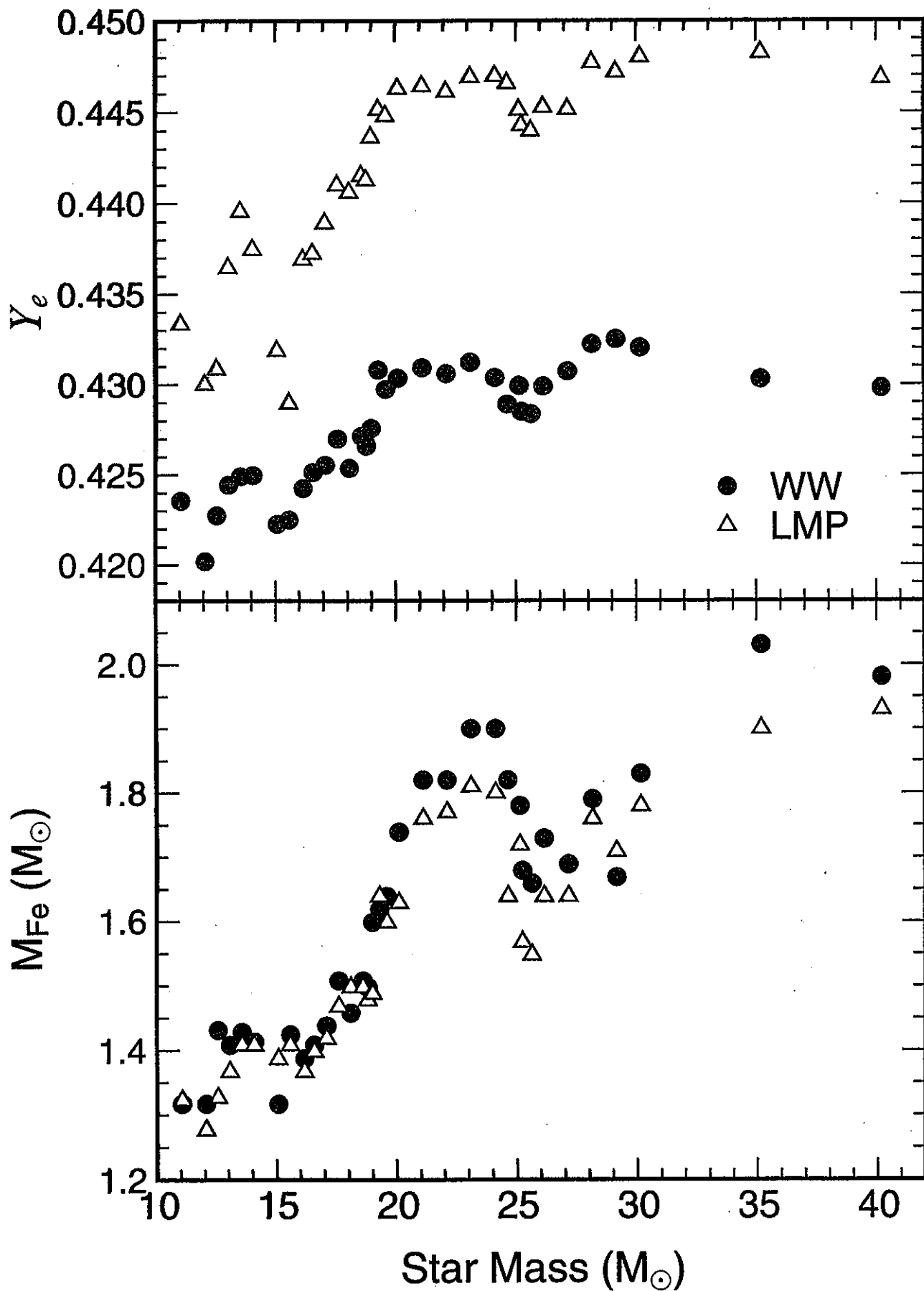
$^{12}\text{C}(\alpha, \gamma)^{16}\text{O}$

treatment of convection

overshooting, semi convection

Coulomb effects on EOS

electron - capture rate



* delayed explosion

衝撃波背面の加熱領域を通過するニュートリノフラックス

neutrino energy	$\propto T_\nu$
neutrino number flux	$\propto T_\nu^3$
absorption cross section	$\propto T_\nu^2$

$$\text{heating rate} \propto T_\nu^6 \propto L_\nu T_\nu^2$$

delayed explosion model はニュートリノフラックスに敏感

(例: Janka and Müller 1993)

- Soft EOS

$$\begin{aligned} E_{\text{bind}}(NS) &\nearrow \Rightarrow \int L_\nu dt \nearrow \\ \rho &\nearrow \Rightarrow T_\nu \nearrow \end{aligned}$$

- Opacity $\Rightarrow L_\nu(t), T_\nu(t)$
 $\int L_\nu(t) dt$: unchanged

初期段階で high L_ν 、high T_ν が好ましそう
 \Rightarrow small opacity is better?

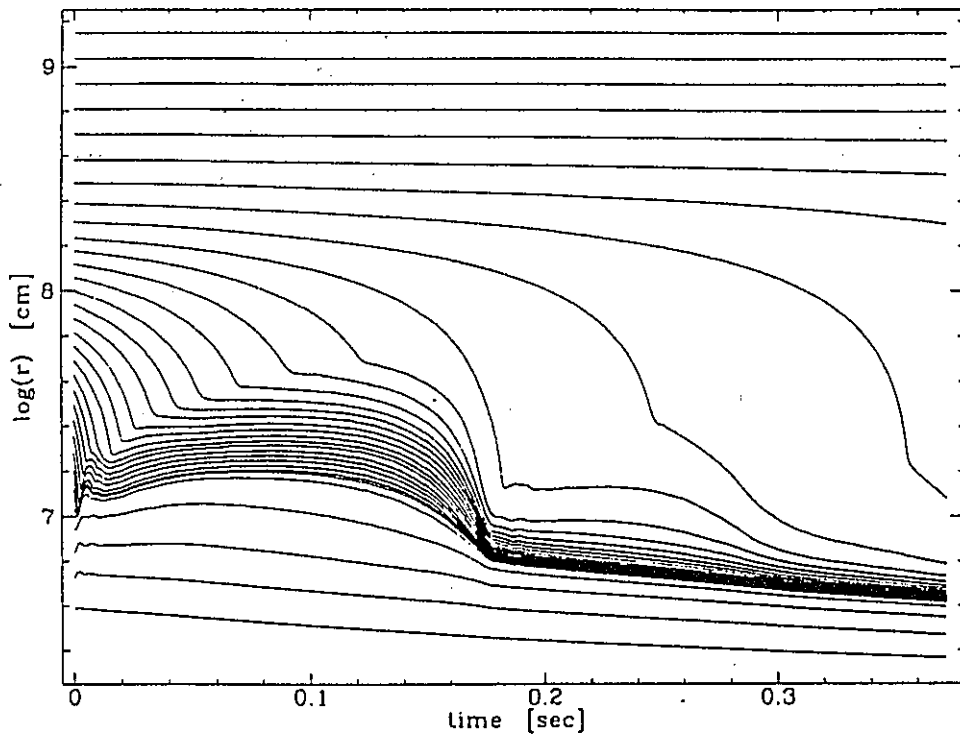
- PNS 内の対流

熱く lepton-rich な物質を、表面近くへ運ぶ
 $\Rightarrow L_\nu \nearrow T_\nu \nearrow$

Wilson の delayed explosion のシミュレーションでも対流の効果を考慮しないと、爆発のエネルギーが足りない。
 対流がどこでどのくらいの規模でおこるのか?

$$\begin{aligned} S(r), Y_L(r) \\ \left(\frac{\partial \rho}{\partial \ln Y_L} \right)_{S,P} \quad (\text{EOS に依存}) \end{aligned}$$

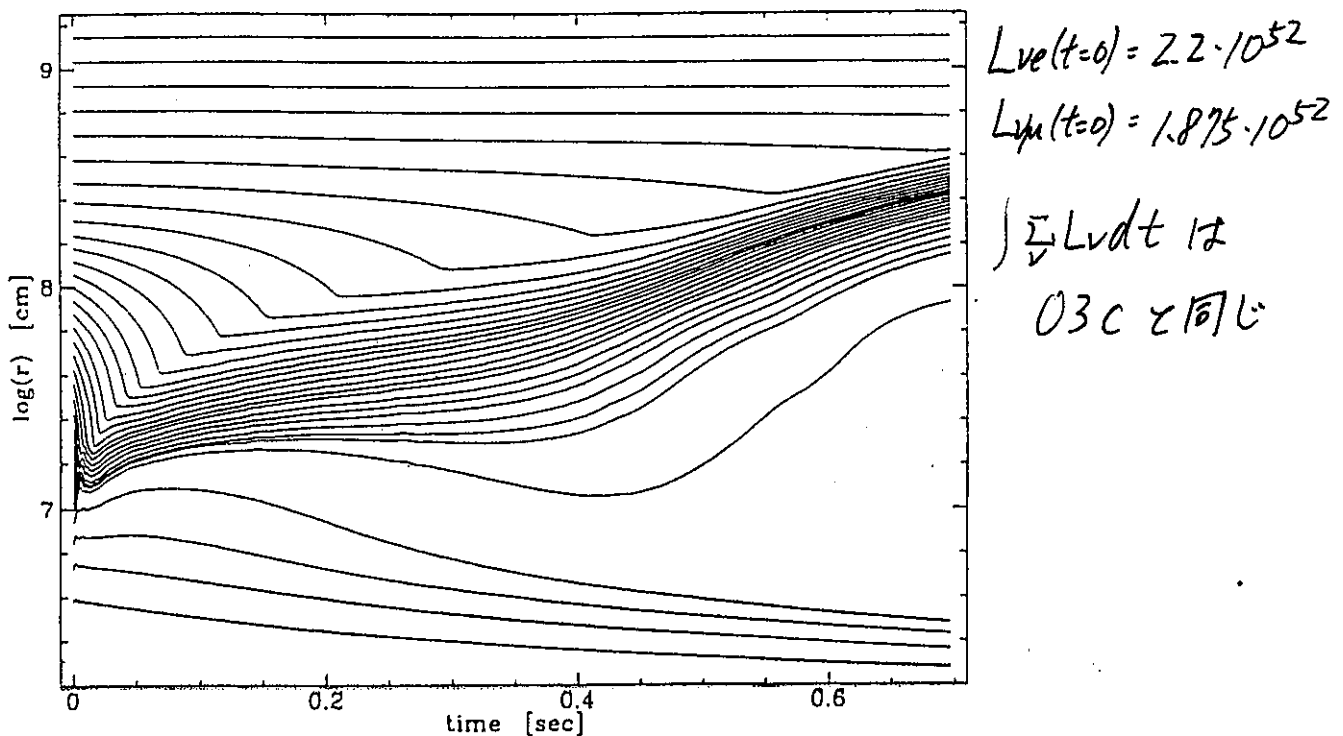
Newtonian hydrodynamics



$$L_{\nu e}(t=0) = 2 \cdot 1 \cdot 10^{52} \text{ erg/s}$$

$$L_{\nu \mu}(t=0) = 1.85 \cdot 10^{52}$$

Fig. 1. Radial positions as functions of time for a sample of mass shells of model O3c (see Table 1). The protoneutron star is sitting at the bottom of the figure, and the position of the supernova shock can be identified at the sharp turns of the curves. The shock exhibits an oscillatory motion and the model does not explode.



$$L_{\nu e}(t=0) = 2.2 \cdot 10^{52}$$

$$L_{\nu \mu}(t=0) = 1.875 \cdot 10^{52}$$

$$\int \sum L_v dt \approx 12$$

$$O3C \times 10^7 L_\odot$$

Fig. 2. Radial positions $r(t)$ for a sample of mass shells of model O4c (see Table 1). After about 400 ms post bounce a strong bifurcation between protoneutron star and stellar mantle develops and the model explodes.

Opacity: ニュートリノ反応率の見直し

- ion screening (Horowitz 1997, Bruenn and Mezzacappa 1997)
Coulomb effect → ions in correlated states
 $\sigma(\nu A \rightarrow \nu A)$ decreases when the wave length of neutrinos > ion separation
コアの重力崩壊のシミュレーション (Bruenn and Mezzacappa 1997)

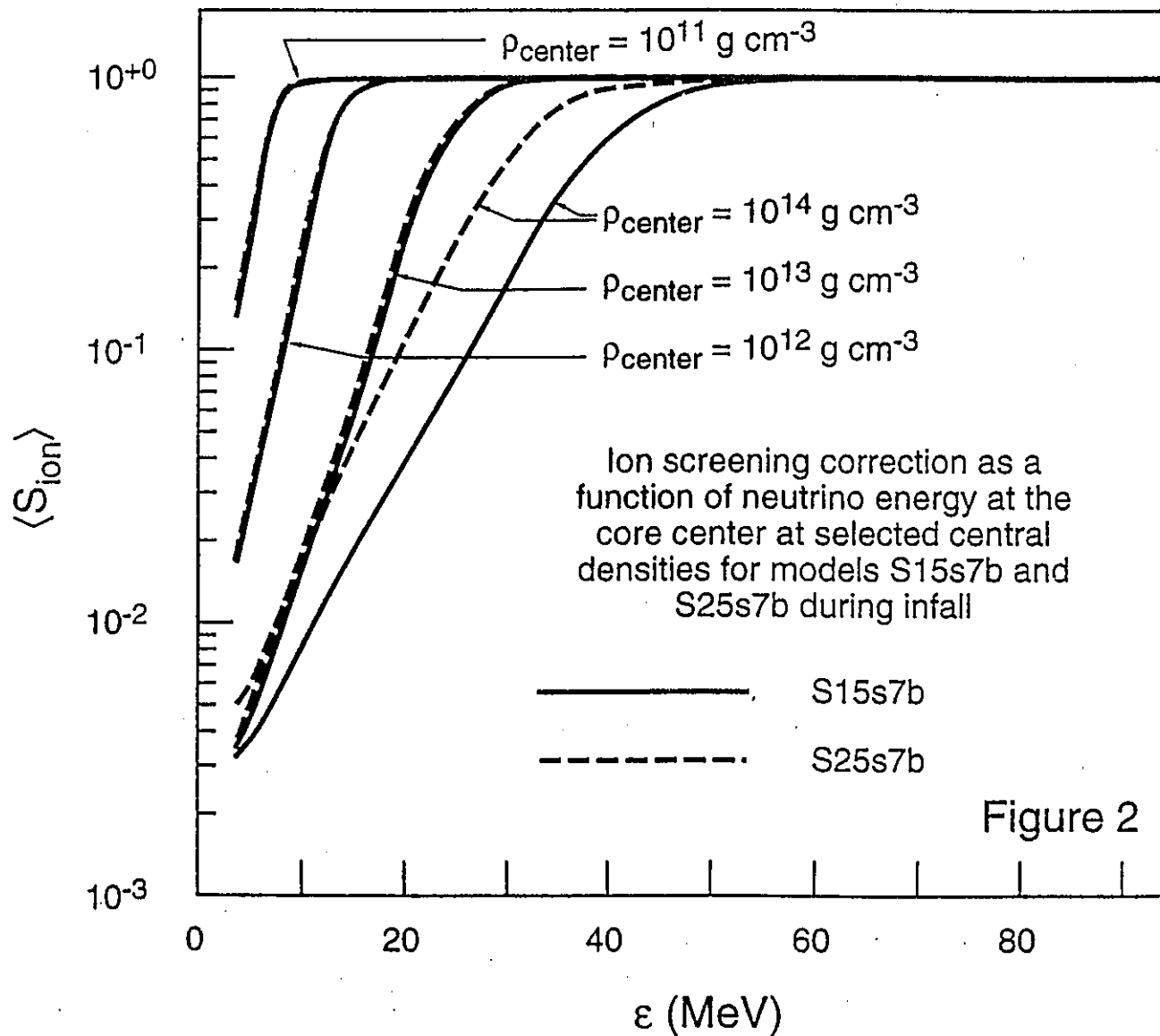
$$\Delta Y_{L\text{trap}} = -0.015 \text{ not so drastic}$$

(narrow ω_ν window is affected)

$$Y_{L\text{trap}} \searrow \Rightarrow M_{\text{i.c.}} \searrow (2 - 6\%) \Rightarrow E_{\text{shock}} \searrow$$

- effective mass, nucleon density/spin fluctuations
⇒ reduction of opacity
(Sawyer 1995, München group 1995-1998, Burrows and Sawyer 1998-1999, Reddy *et al.* 1998-1999, Yamada and Toki 1999-2000)
- 核子制動輻射 $NN' \longleftrightarrow NN' \nu \bar{\nu}$
Suzuki and Ishizuka: One Pion Exchange model
低エネルギーニュートリノを enhance
一方 multiple scattering suppression (Raffelt and Seckel 1991) は低エネルギーニュートリノの核子制動輻射を抑制
(Hannestad and Raffelt, Raffelt and Seckel 1998, Shen and Suzuki, Burrows *et al.* 2000)

多体効果は状態方程式と密接に関連



Burrows & Sawyer '98

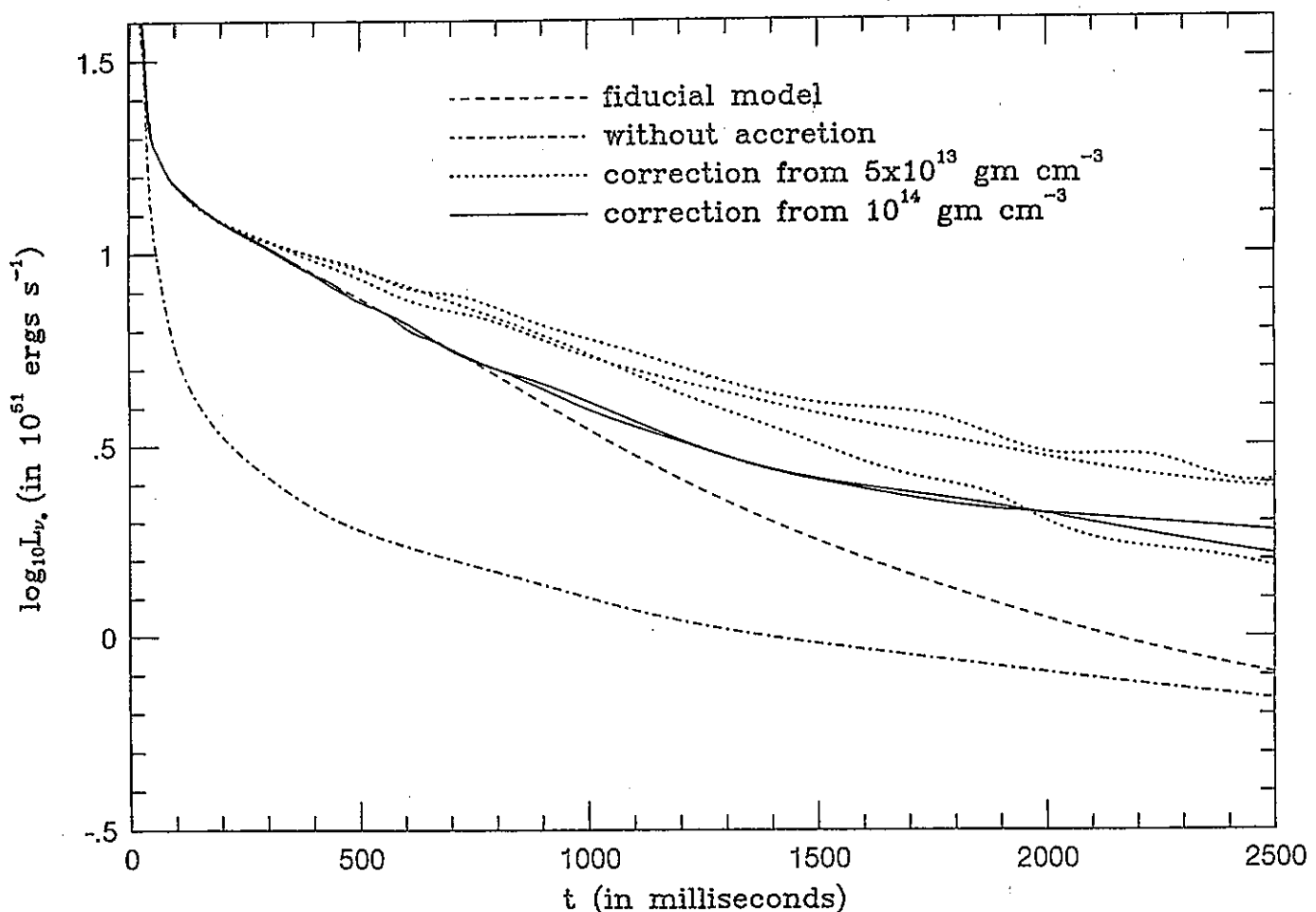


FIG. 11. \log_{10} of the electron neutrino luminosity (L_{ν_e}) in units of 10^{51} ergs s $^{-1}$ versus time after bounce in milliseconds, with and without accretion. For the accretion models, total opacity suppression factors of 0.3, 0.1, and 0.05 were assumed above 5×10^{13} gm cm $^{-3}$ and of 0.3 and 0.1 were assumed above 10^{14} gm cm $^{-3}$. The fiducial model is dashed, the model without accretion is dot-dashed, the models with correction above 5×10^{13} gm cm $^{-3}$ are dotted, and those with correction above 10^{14} gm cm $^{-3}$ are solid. On this plot, the models with the largest corrections have the highest luminosities after 2500 milliseconds. The comparisons between the dashed curve and all others are the most germane.

- ニュートリノ輸送
1D (球対称モデル)

1. Boltzmann solver

$$\frac{df_\nu(t, r, \omega, \mu)}{dt} = \dots$$

radial flow + Doppler shift + gravitational red shift + bending + neutrino interaction

2. MGFLD (multigroup flux limited diffusion scheme)

$$\frac{dn_\nu(t, r, \omega)}{dt} = \dots$$

3. EIFLD (energy-integrated flux limited diffusion scheme)

$$\frac{dn_\nu(t, r)}{dt} = \dots$$

- 状態方程式 (EOS)

$$\left. \begin{array}{l} U(\rho, S, Y_e) \\ P(\rho, S, Y_e) \\ T(\rho, S, Y_e) \\ \mu_i(\rho, S, Y_e) \\ X_i(\rho, S, Y_e) \\ A(\rho, S, Y_e) \\ Z(\rho, S, Y_e) \\ i = n, p, \alpha, A \end{array} \right\} \rightarrow \begin{array}{l} \text{hydrodynamics} \\ \text{neutrino interaction rate} \end{array}$$

一般相対論的効果は重要であるが、1D 計算の一部・2D/3D 計算のほとんどは、これを無視したり、粗く扱っている。

ニュートリノ輸送の計算方法とニュートリノ加熱

$$\text{ニュートリノによる加熱率 } \dot{Q} \propto u_\nu \langle \omega_\nu^2 \rangle \propto \frac{L_\nu}{r^2 \langle \mu \rangle} \langle \omega_\nu^2 \rangle$$

MGFLD(Multi Group Flux Limited Diffusion) 方式は、
計算の外部境界で $\langle \mu \rangle = 1$ となるようになっている。

⇒ $\langle \mu \rangle$ を過大評価

⇒ ニュートリノ加熱率を過小評価

⇒ ボルツマン方程式直接解法による精度の高い加熱率の評価が必要

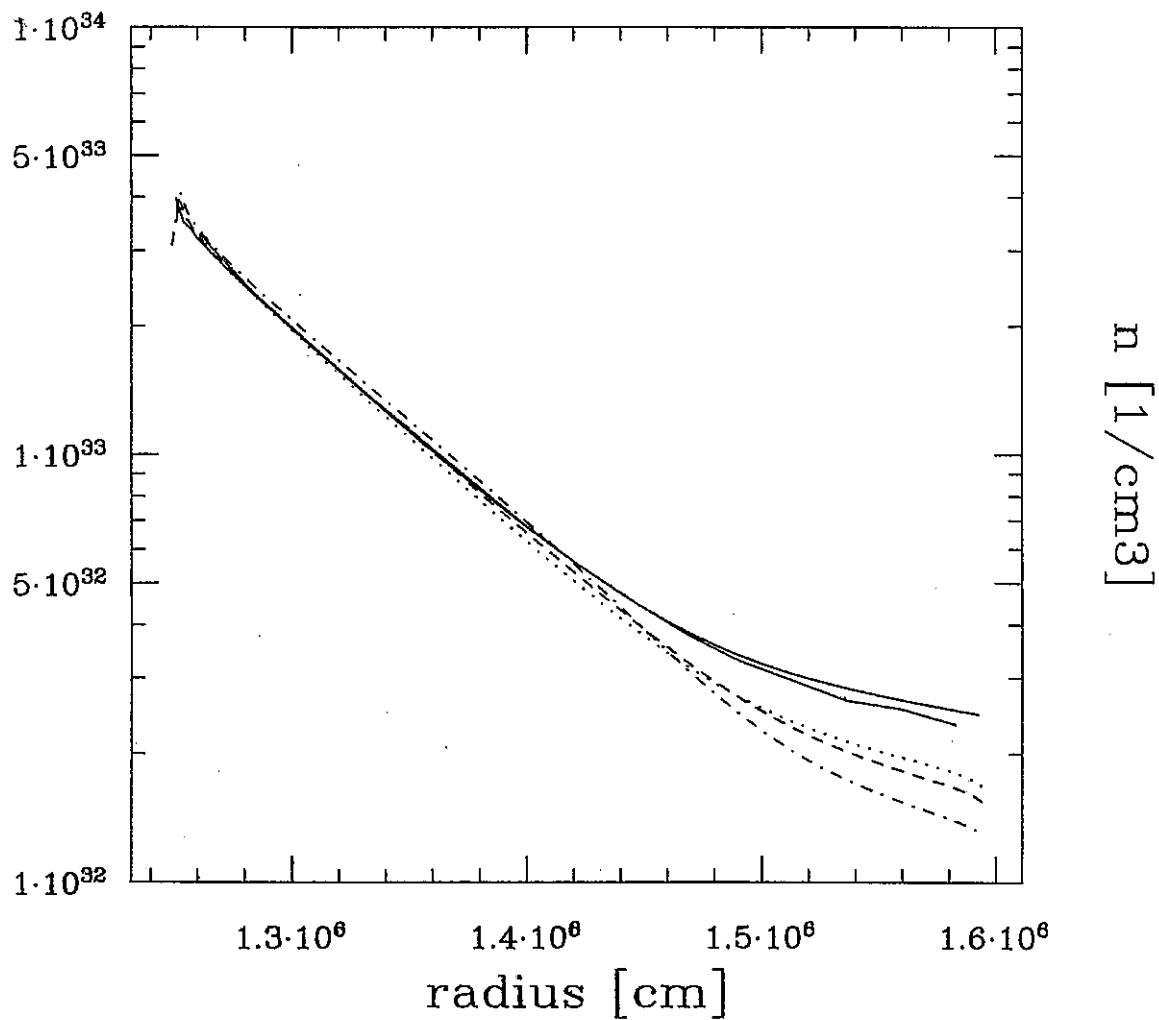
— Bnueb3.32.dat

- - - Dnueb3.32BR7.dat

..... Dnueb3.32LP7.dat

- - - Dnueb3.32MW7.dat

— MCnueb3.32.dat



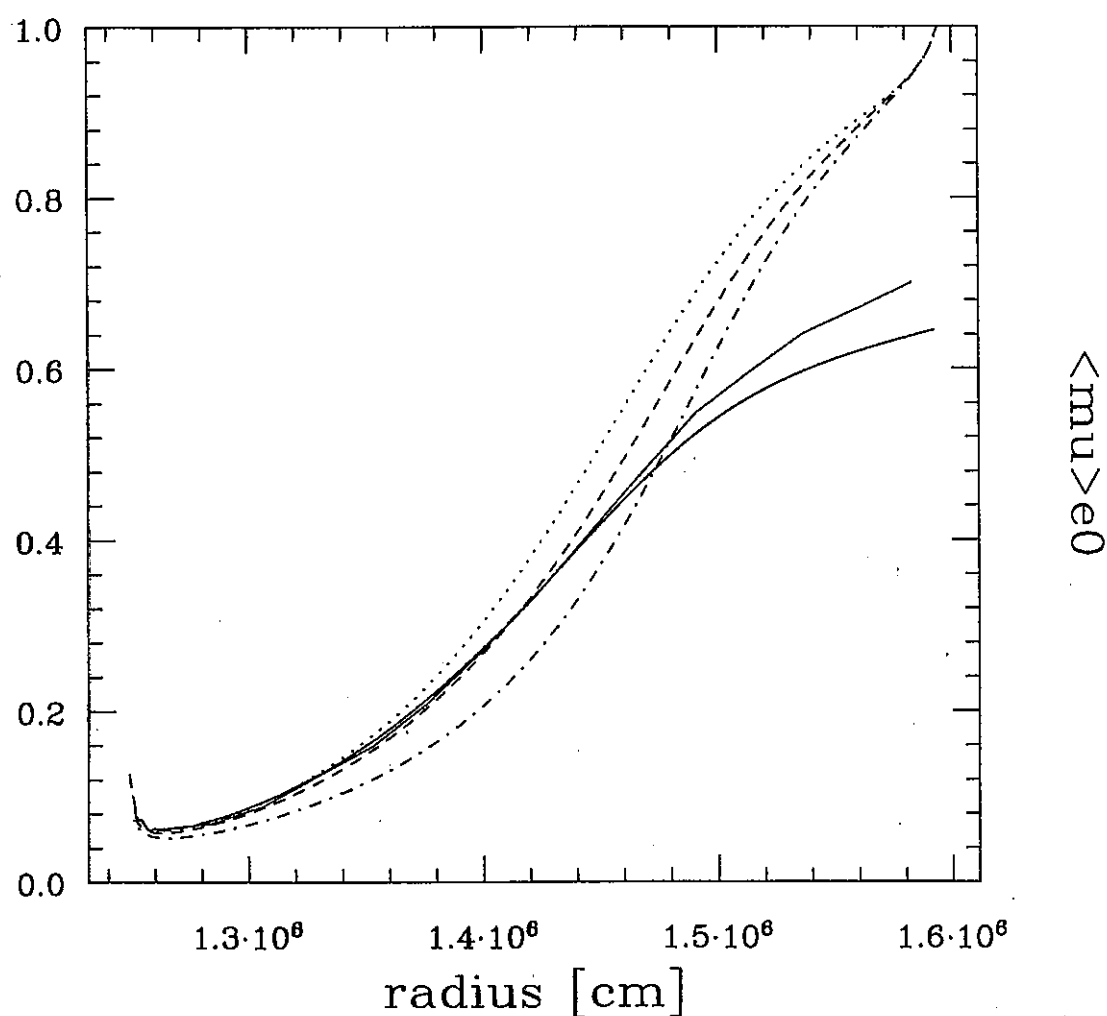
Bnueb3.32.dat

Dnueb3.32BR7.dat

Dnueb3.32LP7.dat

Dnueb3.32MW7.dat

MCnueb3.32.dat



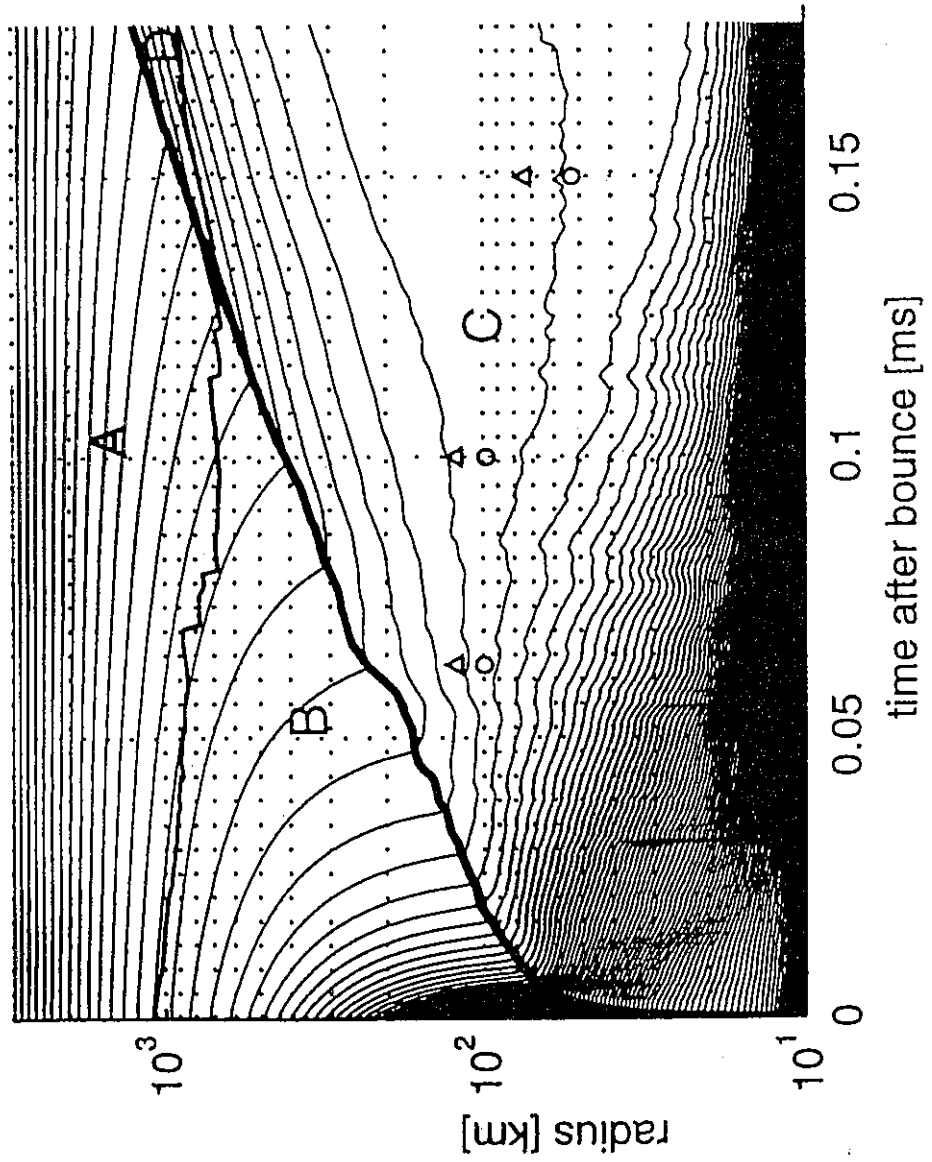


FIG. 4. Radial trajectories of equal mass shells ($0.01 M_{\odot}$) in the iron core and silicon layer. We trace the shock, nuclear burning, and dissociation fronts, which carve out four regions in the (r, t) plane. A: Silicon. B: Iron produced by infall compression and heating. C: Free nucleons and alpha particles. D: Iron and alpha particles produced by shock compression and heating. At three select times, the gain radii (circles) and radii of peak neutrino heating (triangles) are shown.

ニュートリノ振動の天体物理学的な影響

- delayed explosion

$$\rho(\nu\text{sphere}) \sim 10^{12} \text{g/cm}^3 > \rho_{\text{res}} > \rho(\text{hot bubble}) \sim 10^5 \text{g/cm}^3$$

$$1\text{eV}^2 < \Delta m^2 < 10^6 \text{eV}^2$$

$$\nu_{\mu/\tau} \leftrightarrow \nu_e \Rightarrow \langle \omega_{\nu_e}(\text{h.b.}) \rangle \nearrow \text{加熱率} \nearrow \text{delayed explosion} \nearrow$$

- r-process in ν -driven wind

$\langle \omega_{\nu_e} \rangle < \langle \omega_{\bar{\nu}_e} \rangle$ ならば $\nu_e n \rightarrow p e^-$ と $\bar{\nu}_e p \rightarrow n e^+$ がつりあう $Y_e < 0.5$
 \Rightarrow r-process 元素合成

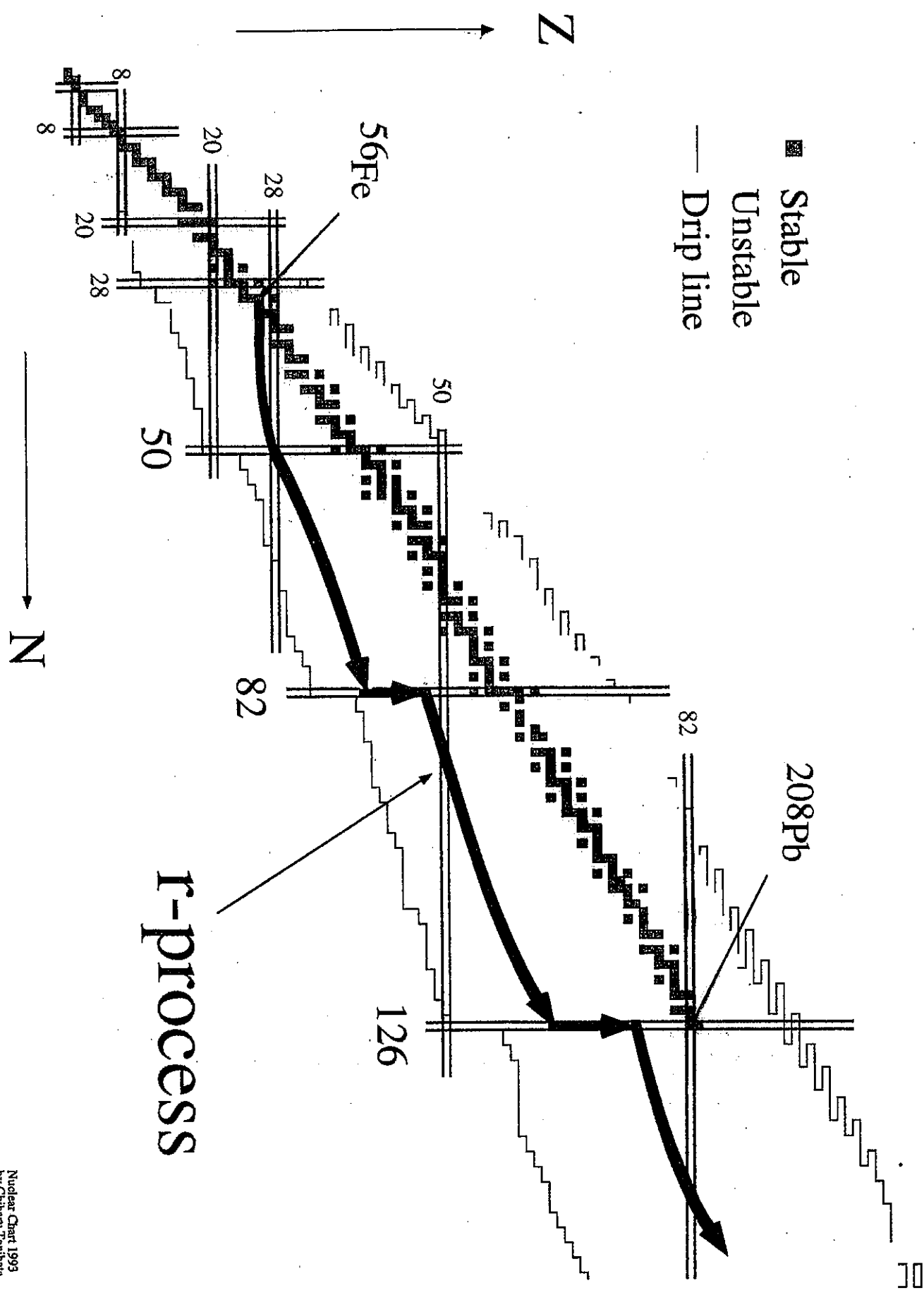
$$\rho(\nu\text{sphere}) \sim 10^{12} \text{g/cm}^3 > \rho_{\text{res}} > \rho(\nu\text{-wind}) \sim 10^5 \text{g/cm}^3$$

$$1\text{eV}^2 < \Delta m^2 < 10^6 \text{eV}^2 \text{ ならば、}$$

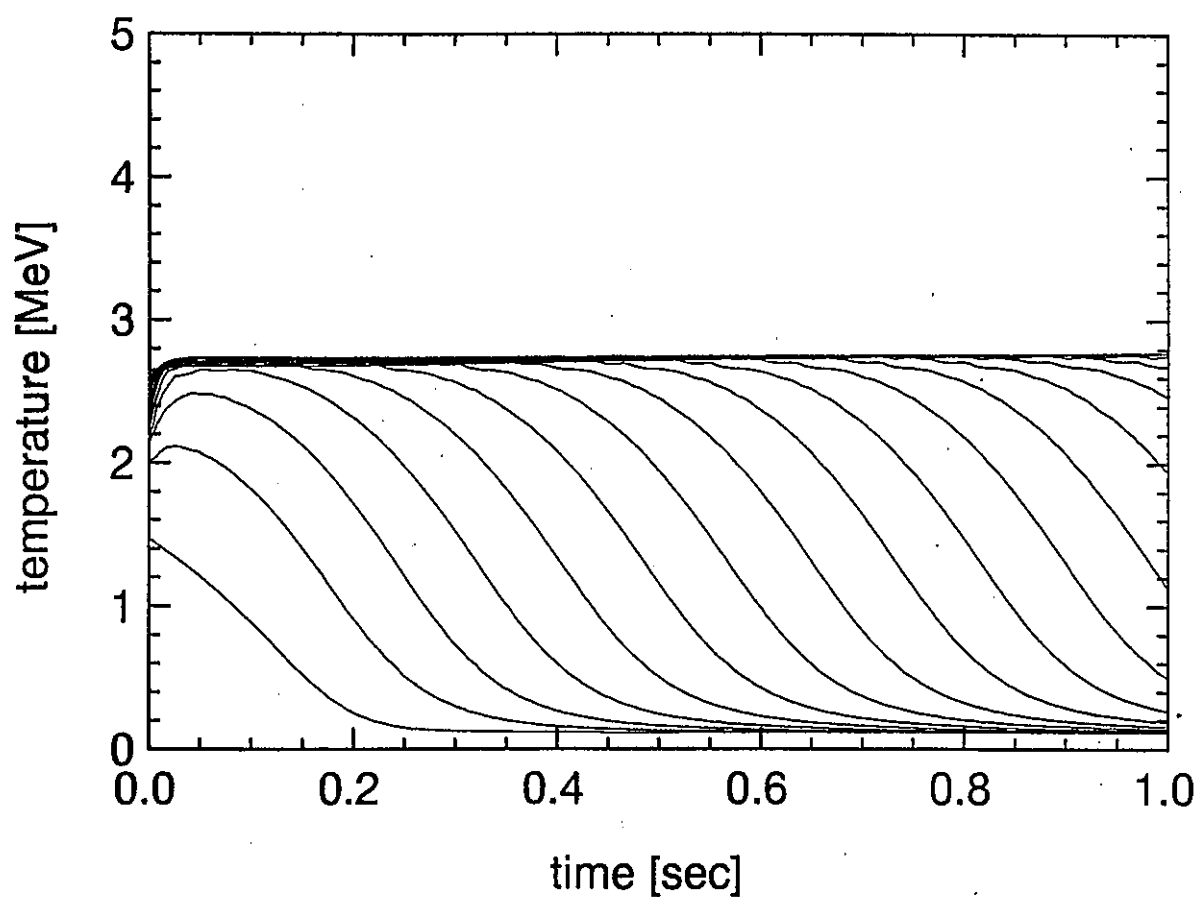
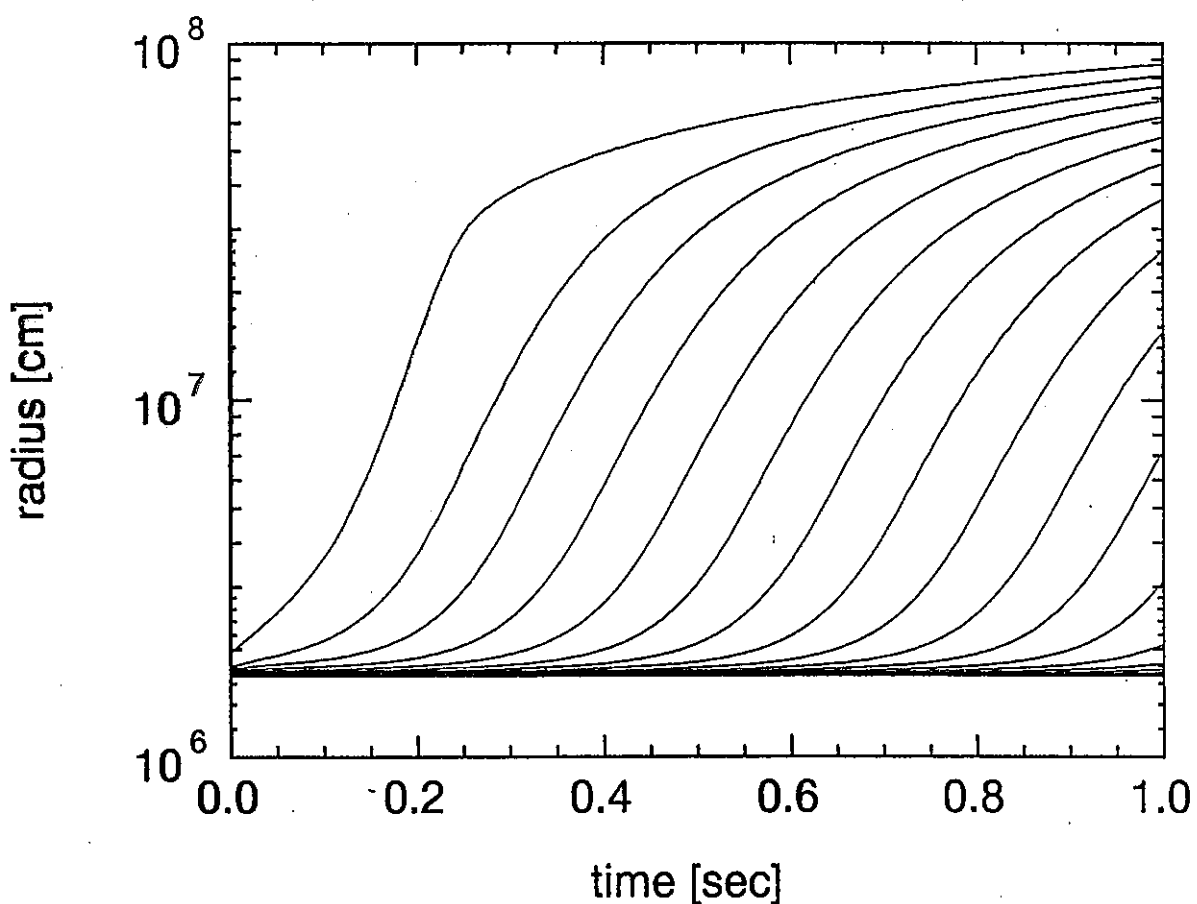
$$\nu_{\mu/\tau} \leftrightarrow \nu_e \Rightarrow \langle \omega_{\nu_e}(\nu\text{-wind}) \rangle \sim \langle \omega_{\nu_{\mu/\tau}}(\nu\text{sphere}) \rangle > \langle \omega_{\bar{\nu}_e}(\nu\text{-wind}) \rangle$$

$Y_e \nearrow \text{r-process} \searrow$
 $\text{heating rate} \nearrow \text{r-process} \nearrow$

- 中性子星の kick velocity



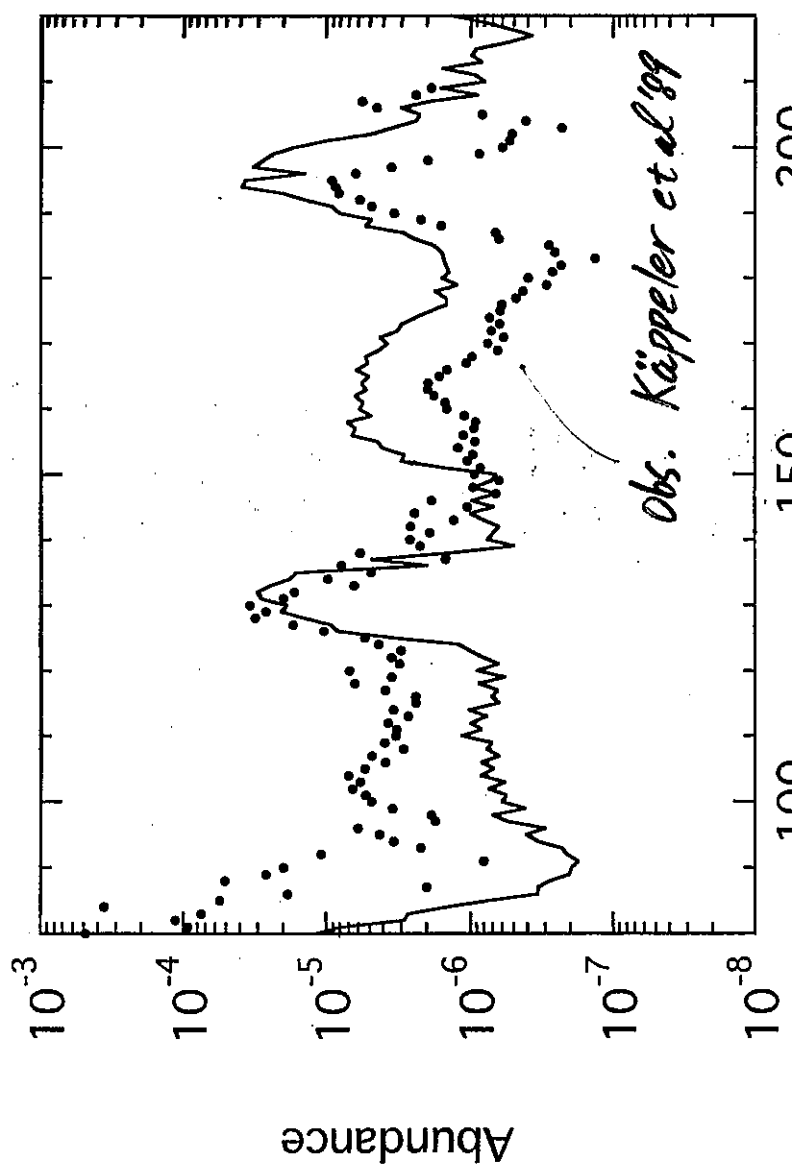
ν -driven wind (Sumiyoshi et al.)



$$M_{\odot} = 1.4 M_{\odot} \quad R = 10 \text{ km} \quad L_{\nu}^{\text{tot}} = 6.0 \cdot 10^{51} \text{ erg/sec}$$

V-driven wind (Sumiyoshi et al.)

Figure 9



$M_{\odot} = 2.0 M_{\odot}$, $R = 10 km$, $L_V^{tot} = 6 \cdot 10^{52} erg/sec$

SN1987A の観測データ

- $\nu_{\mu/\tau} \leftrightarrow \nu_e$

$$\sigma(\nu_{\mu/\tau} e^- \rightarrow \nu_{\mu/\tau} e^-) \sim \frac{1}{7} \sigma(\nu_e e^- \rightarrow \nu_e e^-)$$

$\Rightarrow \nu_e$ の中性子化バーストに伴う前方散乱イベントが減少

KAMIKANDE-II 1st event: $18 \pm 18\text{deg}$

中性子化バーストのモデルから期待される前方散乱イベント数 < 0.1
等方散乱イベントが $18 \pm 18\text{deg}$ に入る確率 ~ 0.05

振動の有無についての議論は無理

- $\bar{\nu}_{\mu/\tau} \leftrightarrow \bar{\nu}_e$ (例えば LMA 解)

Jegerlehner *et al.* 1996

$$\langle \omega_{\bar{\nu}_e} \rangle_{\text{obs}} \sim \langle \omega_{\bar{\nu}_e} \rangle_{\text{theory}} < \langle \omega_{\bar{\nu}_{\mu/\tau}} \rangle_{\text{theory}}$$

$\bar{\nu}_{\mu/\tau} \leftrightarrow \bar{\nu}_e$ は起こっていない

現在の超新星モデルは $\langle \omega_{\bar{\nu}_{\mu/\tau}} \rangle_{\text{theory}}$ を過高評価

超新星モデルの再検討

ニュートリノ反応率、状態方程式、計算手法、多次元化

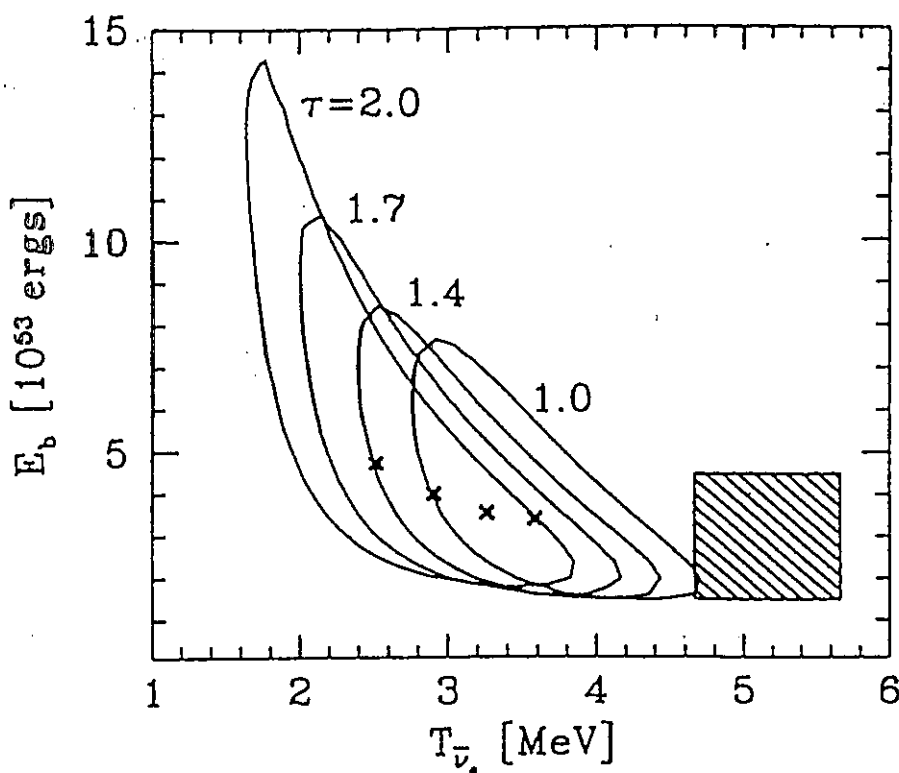


FIG. 10. Best-fit values for $T_{\bar{\nu}_e}$ and E_b and contours of constant likelihood which correspond to 95.4% confidence regions. In each case a joint analysis between both detectors was performed with $\sin^2 2\Theta_0 = 0.8$ and $\Delta m^2 = 10^{-5}$ eV². The curves are marked with the relative $\bar{\nu}_\mu$ temperature τ . The hatched region corresponds to the theoretical predictions of Eqs. (1) and (2).